

# The Decorah structure, northeastern Iowa: Geology and evidence for formation by meteorite impact

Bevan M. French<sup>1,†</sup>, Robert M. McKay<sup>2,§</sup>, Huaibao P. Liu<sup>2,†</sup>, Derek E.G. Briggs<sup>3,†</sup>, and Brian J. Witzke<sup>4,†</sup>

<sup>1</sup>Department of Paleobiology, Smithsonian Institution, Washington, D.C. 20013-7012, USA

<sup>2</sup>Iowa Geological Survey, IHR—Hydroscience & Engineering, University of Iowa, 340 Trowbridge Hall, Iowa City, Iowa, 52242, USA

<sup>3</sup>Department of Geology and Geophysics, and Yale Peabody Museum of Natural History, Yale University, New Haven, Connecticut 06520, USA

<sup>4</sup>Department of Earth and Environmental Sciences, University of Iowa, 121 Trowbridge Hall, Iowa City, Iowa 52242, USA

## ABSTRACT

The Decorah structure, recently discovered in northeastern Iowa, now appears as an almost entirely subsurface, deeply eroded circular basin 5.6 km in diameter and ~200 m deep, that truncates a near-horizontal series of Upper Cambrian to Lower Ordovician platform sediments. Initial analysis of geological and well-drilling data indicated characteristics suggestive of meteorite impact: a circular outline, a shallow basin shape, discordance with the surrounding geology, and a filling of anomalous sediments: (1) the organic-rich Winneshiek Shale, which hosts a distinctive fossil Lagerstätte, (2) an underlying breccia composed of fragments from the surrounding lithologies, and (3) a poorly known series of sediments that includes shale and possible breccia. Quartz grains in drill samples of the breccia unit contain abundant distinctive shock-deformation features in ~1% of the individual quartz grains, chiefly planar fractures (cleavage) and planar deformation features (PDFs). These features provide convincing evidence that the Decorah structure originated by meteorite impact, and current models of meteorite crater formation indicate that it formed as a complex impact crater originally ~6 km in diameter. The subsurface characteristics of the lower portion of the structure are not well known; in particular, there is no evidence for the existence of a central uplift, a feature generally observed in impact structures of comparable size. The current estimated age of the Decorah structure (460–483 Ma) suggests that it may be associated with a group of Middle Ordovician impact craters (a terrestrial “im-

act spike”) triggered by collisions in the asteroid belt at ca. 470 Ma.

## INTRODUCTION

During the past few decades, impacts of large extraterrestrial objects onto the Earth’s surface have become recognized and generally accepted as an important geological process (Grieve, 1991, 1997, 1998, 2001; French, 1998, 2004; Lowman, 2002; Jourdan and Reimold, 2012; Osinski and Pierazzo, 2013). It has also been recognized that these rare but highly energetic events can produce major and often widespread geological effects, including the near-instantaneous formation of large geological structures, the generation of large igneous bodies, the creation of economic mineral and petroleum deposits, the deposition of regional and even global ejecta layers, and (in at least one case) the production of a major biological extinction (at the Cretaceous–Paleogene boundary, 66 Ma; Schulte et al., 2010).

This recognition of terrestrial impact craters and their effects has been based mainly on distinctive and permanent petrographic and geochemical effects produced in target rocks and minerals by the extreme and highly transient conditions of pressure, temperature, stress, and strain generated by the intense shock waves uniquely created by hypervelocity impact events (French and Short, 1968; French, 1998; French and Koeberl, 2010; Koeberl, 2014). In practice, one of the most widespread and widely used criteria for the identification of shock waves and meteorite impact structures has been the multiple sets of narrow, closely spaced lamellae (planar deformation features [PDFs]) developed in quartz (see papers in French and Short [1968]; also Stöffler and Langenhorst, 1994; Grieve et al., 1996; Ferrière et al., 2009), although a small number of other criteria (e.g., megascopic shatter cones and unique geochemical signatures of

the impacting projectile) can also provide unambiguous identifications of impact structures (Tagle and Hecht, 2006; French and Koeberl, 2010; Koeberl, 2014).

Since the 1960s, the number of established terrestrial meteorite structures has increased steadily at a rate of a few new structures per year (Grieve, 1998), chiefly because the recognition of these shock-metamorphic features (generally shatter cones and PDFs in quartz) has made it possible to identify impact structures that are old, poorly exposed, deeply eroded, buried, or even subjected to post-impact metamorphism. At present, more than 190 preserved impact structures have been definitely identified (Earth Impact Database, 2016), and model calculations suggest that at least several hundred preserved impact structures remain to be discovered on the land areas of the earth (Trefil and Raup, 1990; Grieve, 1991; Stewart, 2011; Hergarten and Kenkmann, 2015).

This growing population of recognized impact structures, and the increasing diversity and complexity displayed by individual structures, have made it possible for current research efforts to expand beyond the simple identification of new structures and to explore more general impact-related problems: the mechanics and complexities of large crater formation, the nature of impact-produced rock deformation, the establishment of new criteria for impact events, the effects of the target geologic setting on impact crater development, and the wider geological and environmental consequences of impact events. However, despite the large number of presently known impact structures and the sophisticated state of current impact research, the field continues to evolve rapidly and unpredictably, and the identification of new impact structures remains an essential source of new data and of new and often unexpected questions.

In this paper, we describe the geology and origin of the Decorah structure, now present

<sup>†</sup>frenchb@si.edu, huaibao-liu@uiowa.edu, derek.briggs@yale.edu, brian-witzke@uiowa.edu.

<sup>§</sup>Corresponding author: rjmckayic@gmail.com.

as a small, isolated circular basin (diameter ~5.6 km) in virtually undeformed Upper Cambrian and Lower Ordovician cratonic strata in northeastern Iowa (Liu et al., 2009; McKay et al., 2010, 2011). This structure, recognized during the investigation of a new Konservat-Lagerstätte, the Winneshiek Lagerstätte (Liu et al., 2006, 2007a), is almost entirely sub-surface, appearing as an area of localized and anomalous sedimentary strata and structural deformation. The basin contains strata unlike those of the surrounding Cambrian through Ordovician rocks (McKay et al., 2010, 2011; Witzke et al., 2011; Wolter et al., 2011). At present, two distinct lithologies are well recognized in the upper portion of the basin-filling sediments: (1) the Winneshiek Shale (Wolter et al., 2011), a greenish-gray to black shale, and (2) an underlying polymict breccia apparently derived from local lithologies (McKay et al., 2010, 2011). A third series of rock types, shale, and possible sandstone breccia, are poorly known from the deeper portions of the basin. The areal extent of the basin is presently defined by the known distribution of the Winneshiek Shale, the uppermost basin-fill unit.

In particular, we report here the results of petrographic and petrofabric examinations of quartz grains from small samples of the subsurface polymict breccia underlying the Winneshiek Shale. We provide evidence that microscopic deformation features in the quartz grains are shock-produced planar fractures (PFs) and PDFs, establishing that the Decorah structure was formed by an extraterrestrial impact. We use hereafter the name “Decorah impact structure,” after the city of Decorah, which overlies 40% of the structure. The name was originally introduced by Kass et al. (2013a, 2013b), following their initial analysis of airborne geophysical survey data collected for the study of Precambrian basement geology in a coincident but much larger study area.

Although generally similar to many known impact structures of comparable size, the Decorah structure reveals some unusual characteristics: (1) it is one of only a small number of impact structures developed entirely in a target of layered sediments, with apparently no involvement of the underlying crystalline basement; (2) it displays no evidence of a *central uplift*, a structural feature generally present in impact structures of comparable size; and (3) it has apparently undergone post-impact erosion of ~300–500 m of originally overlying pre-impact sediments, together with such original impact-produced features as an uplifted crater rim and an ejecta layer that surrounded the original structure.

## GEOLOGY OF THE DECORAH STRUCTURE

### Regional Geology, Target Rocks, and Age

The Decorah structure is located in Winneshiek County, northeastern Iowa (Fig. 1); its center is located at latitude  $43^{\circ}18'49''$  and longitude  $91^{\circ}46'19''$ . The structure lies within the Paleozoic Plateau landform region of Iowa, an area of relatively high topographic relief and thin Quaternary deposits lying upon Paleozoic bedrock (Prior, 1991). The upper surface of the structure, currently best defined by the mostly subsurface distribution of the Winneshiek Shale, spans a circular area of ~24.8 km<sup>2</sup>. About 10.1 km<sup>2</sup> of the structure underlies the town of Decorah. The bedrock-entrenched Upper Iowa

River meanders across the southern half of the structure where, on average, 20 m of Quaternary alluvium overlies bedrock. The depth to the top of structure varies from 0 m at the river level outcrop of the Winneshiek Shale near the structure's eastern edge to 111 m along the northwestern margin on the upland above the river valley.

Paleozoic bedrock in the region is a gently tilted sequence of Upper Cambrian through Upper Ordovician cratonic sedimentary strata (Table 1), chiefly quartzose and fine-grained feldspathic arenites, carbonate rocks, and lesser shale (Witzke and McKay, 1987; Witzke and Glenister, 1987; McKay, 1988, 1993; Ludwigson and Bunker, 2005; Runkel et al., 1998, 2007, 2008; Wolter et al., 2011). The maximum thickness of Paleozoic strata is estimated from

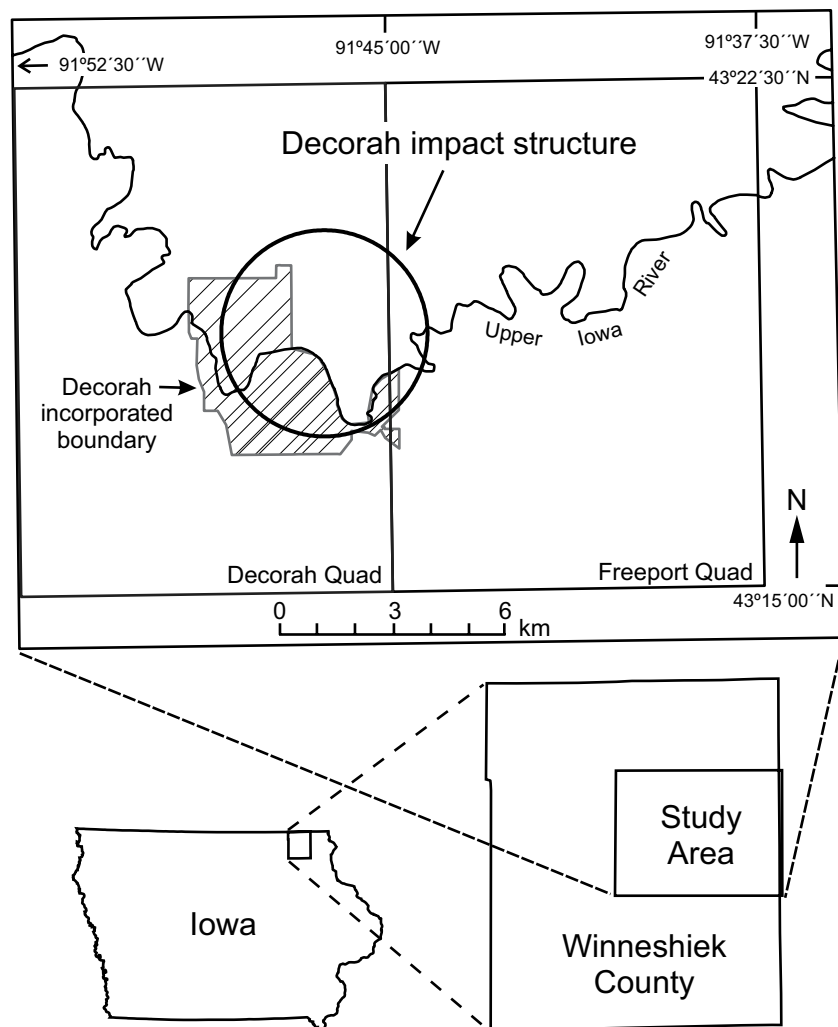


**Figure 1.** Location map showing the Decorah impact structure in Winneshiek County, northeastern Iowa. Inset maps show details of the 385 km<sup>2</sup> study area, the Decorah impact structure, the incorporated limits of the city of Decorah, Iowa, the Upper Iowa River, and the U.S. Geological Survey 7.5 min Decorah and Freeport quadrangles.

TABLE 1. STRATIGRAPHY OF PALEOZOIC UNITS IN THE VICINITY OF THE DECORAH IMPACT STRUCTURE

System	Group/formation	Thickness (m)	Lithology
Upper Ordovician	Maquoketa Formation	35	Limestone and shale
	Galena Group		
	Dubuque Formation	10	Limestone and minor shale
	Wise Lake Formation	21	Limestone, dolomitic, bioturbated
	Dunleith Formation	42	Limestone, dolomitic, cherty
	Decorah Formation	13–14	Shale and limestone, two K-bentonites
	Platteville Formation	8	Limestone
	Glenwood Shale	3	Shale and minor siltstone
Middle Ordovician	St. Peter Sandstone	17–31	Fine- to medium-grained quartzose sandstone
Lower Ordovician	Major unconformity		
	Prairie du Chien Group		
	Shakopee Formation*	19–42	Dolomite, sandy dolomite, and fine- to coarse-grained quartzose sandstone
	Unconformity		
	Oneota Formation*	59–62	Dolomite, cherty
Upper Cambrian	Unconformity		
	Jordan Sandstone*	28–31	Very-fine to coarse-grained feldspathic to quartzose sandstone
	St. Lawrence Formation*	37	Dolomite and dolomitic siltstone, glauconitic
	Lone Rock Formation*	43	Very fine- to fine-grained feldspathic sandstone, shale, minor dolomite, glauconitic
	Wonewoc Formation	40–44	Fine- to coarse-grained quartzose sandstone
	Eau Claire Formation	41–50	Very fine- to fine-grained feldspathic sandstone and shale, minor dolomite, glauconitic
	Mt. Simon Formation	140–180 <sup>†</sup>	Fine- to very coarse-grained quartzose sandstone, minor shale

Note: Thickness values derived from measured sections and well data in Iowa Geological Survey files and publications cited in text.  
 \*Unit is absent from the area within the Decorah impact structure, and is replaced by the Winneshiek Shale and sub-Winneshiek breccia, sandstone and shale.  
<sup>†</sup>Estimated.

drill hole information to be 620 m. Formations dip uniformly to the southwest at an average of 7.2 m/km (<0.5°), a subdued structural attitude typical of the region. Compared to much of Iowa, bedrock exposures, especially along valley walls, are common, but Quaternary colluvium, loess, and patchy glacial till up to a few meters thick mantle large portions of the valley walls and uplands.

The Paleozoic strata are underlain by a Precambrian (Mesoproterozoic) mafic to ultramafic complex thought to intrude Yavapai province (1.8–1.72 Ga) metagabbro and felsic plutons (Drenth et al., 2015). This basement complex is estimated to be present at depths of 490–620 m below the land surface.

Paleozoic formations in the region have primarily been dated using biostratigraphy, but radiometric age dates from three K-bentonites in the overlying Galena Group (Kolata et al., 1996) provide additional age constraints on the structure. Of the three bentonites, the most accurately dated is the Millbrig K-bentonite, 1 m above the base of the Decorah Formation and ~37 m above the top of the Winneshiek Shale. <sup>40</sup>Ar/<sup>39</sup>Ar single crystal laser fusion experiments on sani-

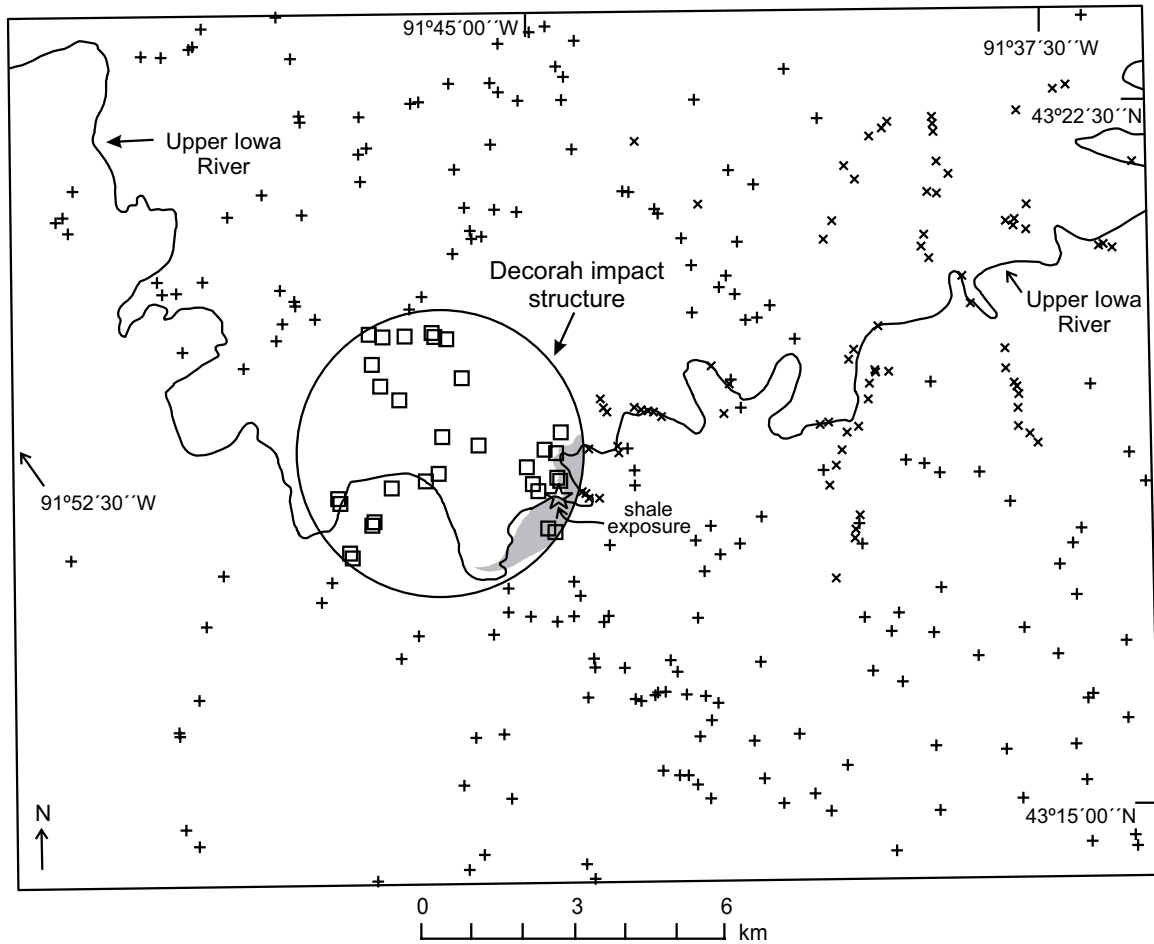
dine phenocrysts from the Millbrig yielded ages of 454–449 Ma (Chetel et al., 2004, 2005; Smith et al., 2011), a Late Ordovician age straddling the Sandbian–Katian stage boundary (Cohen et al., 2013). This figure provides a minimum absolute age for the Decorah structure, but conodonts from both the crater-filling Winneshiek Shale, and the overlying crater-capping St. Peter Sandstone, are likely middle-late Darriwilian (Liu et al., 2017), indicating a minimum age of 460–465 Ma for the Decorah structure. A maximum age is provided by distinctive conodont faunas from the Shakopee Formation, the youngest rock unit currently preserved that is disturbed by the structure. These faunas, part of the North American Midcontinent Province fauna (NAMP), contain elements of Ibexian fauna D (Smith and Clark, 1996), and are representative of the middle Tremadocian. Thus the Decorah structure was formed between the middle Tremadocian and the middle Darriwilian, 460–483 Ma (Cohen et al., 2013). (A recently published study [Bergström et al., 2018] has used  $\delta^{13}\text{C}_{\text{org}}$  chemostratigraphy to estimate the age of the Winneshiek Shale and the Decorah impact structure as 464–467 Ma, values


that are consistent with the other estimates given here.)

### General Features of the Decorah Structure

The approximate areal extent of the Decorah structure is defined chiefly by the occurrence of the unusual Winneshiek Shale (Liu et al., 2006), which is the uppermost basin-filling unit. Occurrences of the shale, identified in one small surface outcrop, water-well drill-cuttings, drillers’ logs, and drill cores (McKay et al., 2010, 2011) define a roughly circular area with a diameter of ~5.6 km (Fig. 2). More than 478 study area well records and 85 outcrops were examined in support of this delineation. Of those records, 35 encounter Winneshiek Shale and 23 sub-Winneshiek breccia. Subsequent airborne transient electromagnetic data identified and mapped the Winneshiek Shale as a circular conductor aligned nearly perfectly with the distribution mapped from the drill hole and outcrop data (Kass et al., 2013a, 2013b). The structure truncates the Cambrian Lone Rock, St. Lawrence, and Jordan formations, and the Ordovician Oneota and Shakopee formations (Fig. 3 and Table 1). The basin, and the rocks that fill it, are almost completely in the subsurface. About 94% (23.4 km<sup>2</sup>) of the structure is disconformably overlain by the St. Peter Sandstone, and ~6% (1.49 km<sup>2</sup>) is unconformably overlain by Quaternary alluvium of the Upper Iowa River. The uppermost basin fill (Winneshiek Shale) and deformed pre-impact target rocks are exposed at the present land surface in two separate small outcrops totaling less than 20 m<sup>2</sup>.

The distribution of Winneshiek Shale (Fig. 2), and the singular occurrence of deformed sedimentary rocks, define a roughly circular structure. Data from well cuttings and drill core samples indicate that this structure is a basin ~210 m in maximum depth, filled completely by a series of unique local lithologies not found in the surrounding sedimentary succession. Data on the substructure of the central portion of the basin are currently confined to a single set of well cuttings (Fig. 3: Well 53572). This information is not sufficient to determine the exact nature of the floor of the structure, the location of the boundary between breccia and underlying bedrock, or the degree of deformation and displacement of the pre-basin sedimentary bedrock units. In particular, there is no indication as to whether or not the Decorah impact structure exhibits a central uplift of the subcrater rocks, a feature typical for impact structures of comparable size (e.g., Grieve, 1991; Grieve and Pilkington, 1996). (See discussion below under “Apparent Absence of a Central Uplift”).



- + well encounters Prairie du Chien Group below the St. Peter Fm., or the first bedrock in well is Prairie du Chien Group
  - well encounters Winneshiek Shale below the St. Peter Fm., or below Quaternary alluvium/colluvium
  - x exposure of Prairie du Chien Group
  - ☆ exposure of Winneshiek Shale and site of H2 core
- 
 subcrop of Winneshiek Shale beneath Quaternary alluvium or colluvium

**Figure 2.** Map showing the locations and types of geologic data (well boreholes, outcrops, subcrop, etc.) used to define the distribution of the Winneshiek Shale. This unit occurs only within a circle ~5.6 km in diameter, labeled “Decorah impact structure”; outside this circle the Winneshiek is absent and the normal stratigraphy is present. The distribution of the Winneshiek Shale is therefore taken as a proxy for the area occupied by the currently preserved basin of the Decorah impact structure. The structure includes locations where the Winneshiek Shale is present at depth but overlain by younger units, such as the St. Peter Sandstone, as well as areas where the Winneshiek Shale is present at the bedrock surface but overlain by Quaternary alluvium, i.e., in the southeast quadrant of the structure.

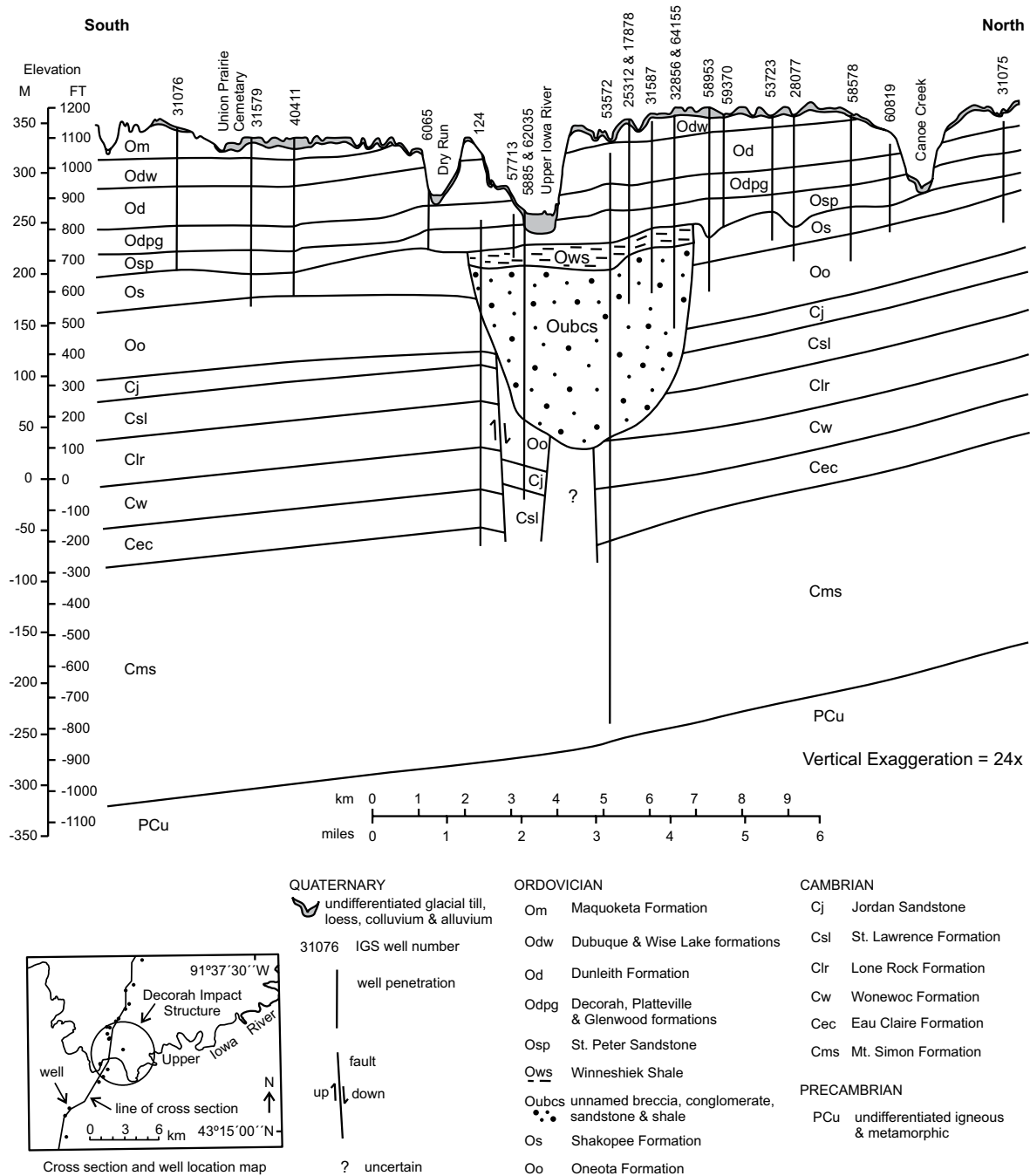


**Figure 3. Geologic cross-section across the study area and through the western portion of the Decorah impact structure. (Orientation approximately north-south [see inset]; cross section hung on elevation; vertical exaggeration 24x.)** The uniformly gentle southwest-erly dips of the regionally widespread Upper Cambrian and Lower Ordovician formations are disrupted by the impact basin (center) and its filling of breccia, conglomerate, and sandstone (Oubcs), which is in turn overlain by a cap of Winneshiek Shale (Ows). Much of the impact basin is disconformably overlain by the St. Peter Sandstone, whose thickness varies considerably because of its disconformable relationship to the Winneshiek Shale and its unconformable relationship to the underlying Shakopee Formation outside the structure. Cuttings from Well 5885, located on the south side of the structure, are interpreted to indicate that the well encountered a down-dropped block of Oneota, Jordan, and St. Lawrence formations below the present crater floor. Cuttings sample logs for all numbered wells are available on the GeoSam section of the Iowa Geological Survey's (IGS) website, <https://www.ihr.uiowa.edu/igs/geosam/home> (accessed April 2018). Minor inconsistencies between this figure and a more detailed cross-section (Fig. 18) are due to: different locations of the two sections within the crater (i.e., this section trends approximately N-S through the western margin of the structure, while the section in Figure 18 trends approximately NW-SE through the center); the use of different drill holes for the different sections; and different presentations of the vertical dimension in the two sections (i.e., as elevation [this figure] and as depth [Fig. 18]). Considering the schematic character of both cross-sections, these inconsistencies are not considered significant.

The Decorah structure is expressed by features of its internal stratigraphy (Figs. 3 and 4): (1) an absence of units within the normal stratigraphy of the area (Lone Rock through Shakopee formations); (2) indications of deformation and down-dropping of the normal sedimentary section; (3) the circular distribution, at the top of the basin,

of the Winneshiek Shale, a distinctive greenish-gray to black shale which contains a striking fossil Lagerstätte and is unknown outside the structure; and (4) the presence of an unusual and thick breccia unit, composed of large and small fragments of several units in the normal stratigraphy, underlying the Winneshiek Shale.

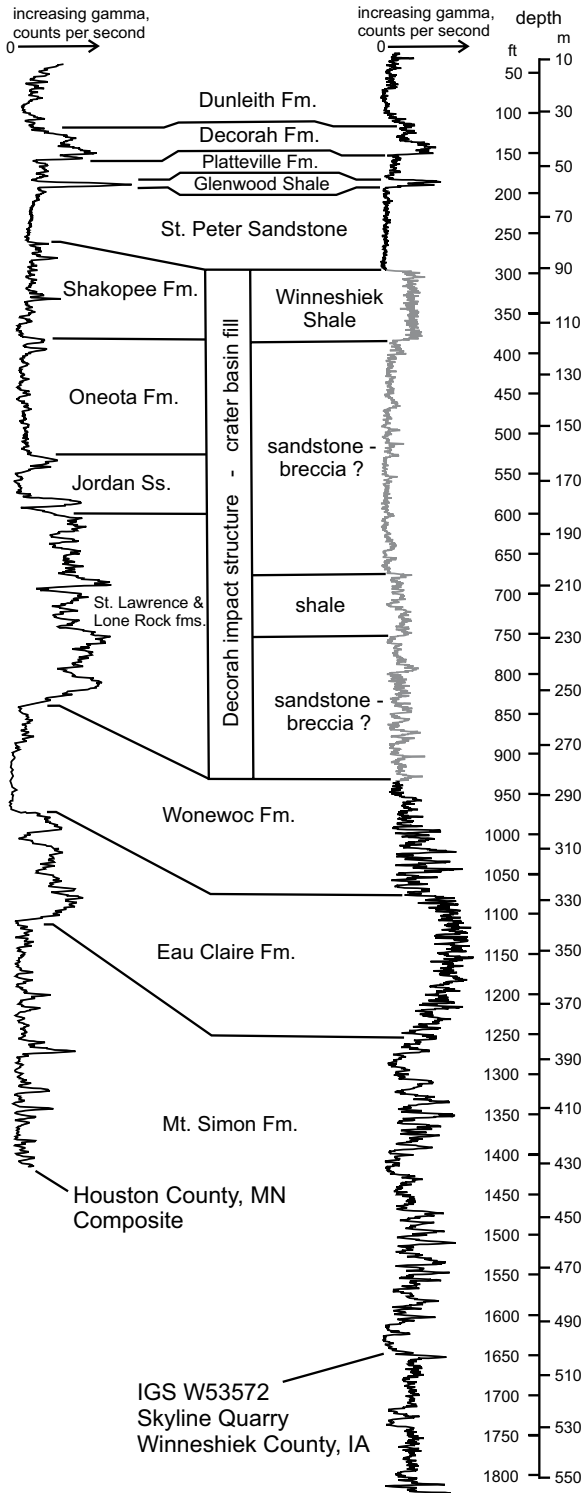


**Figure 4. Gamma-ray intensity logs of stratigraphic units within and outside of the Decorah impact structure.** Left-hand side of the diagram shows a composite natural gamma log for the normal lower Paleozoic formations (fms.) outside the Decorah impact structure, as measured in adjacent Houston County, Minnesota (modified from Runkel, 1996; uses Minnesota Geological Survey gamma logs LaCrescent #4, Zibrowski, and Spring Grove Creamery). Right-hand side of diagram shows the natural gamma log from the deep Skyline Quarry well (53572), located 0.34 km north of the center of the Decorah impact structure. The two logs show relative gamma-ray intensities and are compared using the top of the St. Peter Sandstone (Ss.) as a datum. Note the distinctively higher relative gamma readings of the Winneshiek Shale compared to the Shakopee Formation, and the lower and significantly more uniform relative gamma readings of the sub-Winneshiek breccia compared to the lower Jordan, St. Lawrence, and Lone Rock formations. Relative gamma signatures of the Wonewoc, Eau Claire, and Mt. Simon formations in Well 53572 log are somewhat noisier compared to Houston County. A supporting cuttings sample log for Well 53572 is available on the GeoSam section of the Iowa Geological Survey’s website, <https://www.iihr.uiowa.edu/igs/geosam/home> (accessed April 2018).

**Surface Exposures and Access to Subsurface Crater-Fill Units**

Surface exposures of the units involved in the Decorah structure are limited to one small river-bank exposure of the Winneshiek Shale and one demonstrably deformed and brecciated outcrop of Shakopee Formation. Both exposures occur along the Upper Iowa River at low elevations near the up-dip eastern side of the structure. The Winneshiek Shale exposure is the locality where the Winneshiek fauna has been collected (Liu, et al., 2006, 2007a, 2007b, 2009, 2013, 2017; Lamsdell et al. 2015a, 2015b; Nowak et al., 2017, 2018; Briggs et al., 2016; Hawkins et al., 2018). The H2 core (Figs. 5 and 6) was drilled at this locality above the outcrop.

A single exposure of deformed and brecciated Shakopee dolomite (Fig. 7) was discovered on the grounds of the Oneota Country Club after the basin boundary was mapped. This Shakopee outcrop is located ~50 m east of the boundary, which in this area is buried beneath Upper Iowa River alluvium. The outcrop apparently represents pre-impact target rock just outside the crater boundary, and the dolomite exhibits dips that are steep and irregular; values >10° and possibly up to 55° were noted, in contrast to the dips of <1° that are normal in the region. The outcrop also shows significant deformation (Fig. 7) compared to exposures of the same unit further outside the basin: general and pervasive closely spaced fracturing, multiple subparallel fracture sets, local in-place autobrecciation, possible tight overturned folding, and possible faulting and displacement. No exotic breccias (e.g., intrusive polymict breccia dikes) were observed. Shatter cones, which are features diagnostic of meteorite impact (French and Koeberl, 2010, p. 129) and are often well developed in fine-grained carbonate target rocks, were also not found.

Twenty-three of the 35 drill records that encounter Winneshiek Shale are deep enough to indicate the presence of sub-Winneshiek breccia, but only 18 of those include satisfactory samples of both Winneshiek Shale and sub-Winneshiek breccia. Of those 18 holes, two were cored; the other 16 were drilled as water wells, and drill-cutting chips were routinely collected and saved as samples. Four of the water wells are interpreted to penetrate the entire basin fill; three of these are located near the basin margin (Wells 124, 5885, and 25454) and one near the basin center (Well 53572); the remaining holes penetrate the sub-Winneshiek breccia from 16 to 108 m. All well numbers have been assigned by the Iowa Geological Survey, and all collected samples are permanently stored in the Rock Library.



Figure 5. Graphic core log of the H2 core located 0.32 km inside the mapped eastern basin edge (see Fig. 2), and drilled above the only known outcrop of Winneshiek Shale. The core makes a full penetration of the Winneshiek Shale and a partial penetration of the sub-Winneshiek breccia. The upper portion of the breccia grades upward from breccia into very coarse sandstone, then into finer sandstone with shale interbeds, and finally into the fossiliferous Winneshiek Shale. The contact between the breccia and the overlying Winneshiek shale is placed at a depth of ~18.5 m, at the first appearance of shale; this coincides with the presence of minor burrow traces. The overlying disconformable contact between the Winneshiek Shale and the St. Peter Sandstone (Ss.), at ~2 m depth, is very sharp and displays a truncated and oxidized weathered appearance. A concentration of heavy minerals dominated by ilmenite and zircon, i.e., a heavy mineral lag deposit, was recovered at this contact from the adjacent excavated outcrop. TD—total depth.



The basin fill (Figs. 3, 4, 5, and 6) includes two units of particular significance. A lower (unnamed) breccia unit (Figs. 5 and 6) is composed of large and small, poorly sorted fragments of locally derived carbonates and sandstones; this unit may be partly or completely formed by sedimentary processes. It includes numerous rounded single quartz grains  $\leq 2$  mm in size, of which approximately  $\leq 1\%$  contain planar microstructures (both PFs and PDFs) produced by shock waves and described below. The overlying, clearly sedimentary, Winneshiek Shale varies from ~17–27 m in thickness across the basin, contains the unusual Lagerstätte deposit (Liu et al., 2006), and is itself overlain disconformably by the Ordovician St. Peter Sandstone and Quaternary alluvium.

### Crater-Fill Units: The Crater-Fill Breccia

A presently unnamed and complicated series of possible sediments and/or breccias, so far accessible only from drill cores and drill cuttings, underlies the Winneshiek Shale and apparently fills the remainder of the basin down to a tentatively identified floor of Paleozoic sedimentary bedrock (Figs. 3 and 4). Because the few available coherent samples, obtained from two drill cores, show a highly fragmental and poorly sorted texture (see discussion of Sample H2-1-2, below), this unit is provisionally referred to as “crater-fill breccia,” without considering the de-

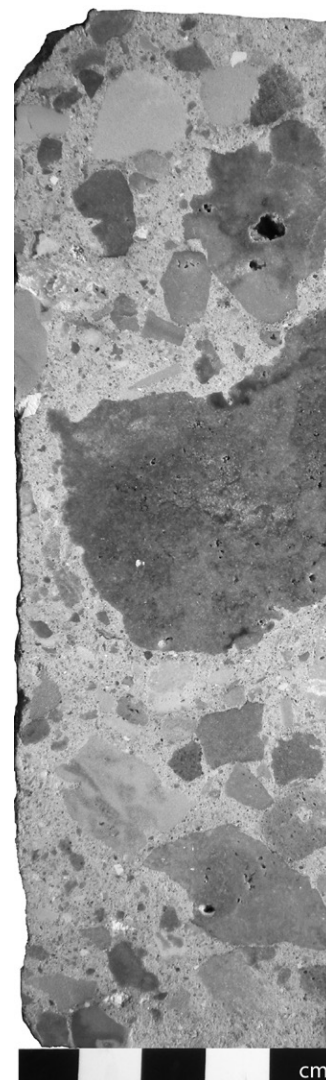
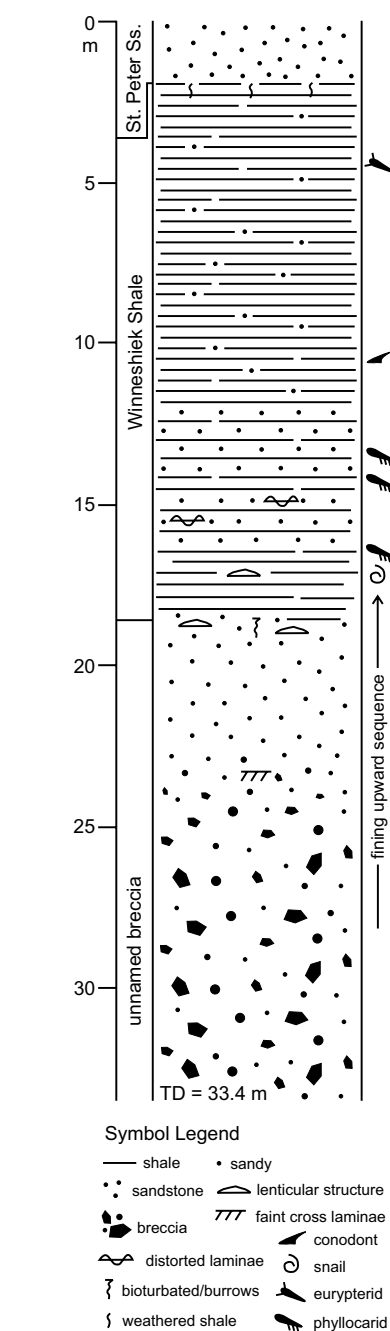
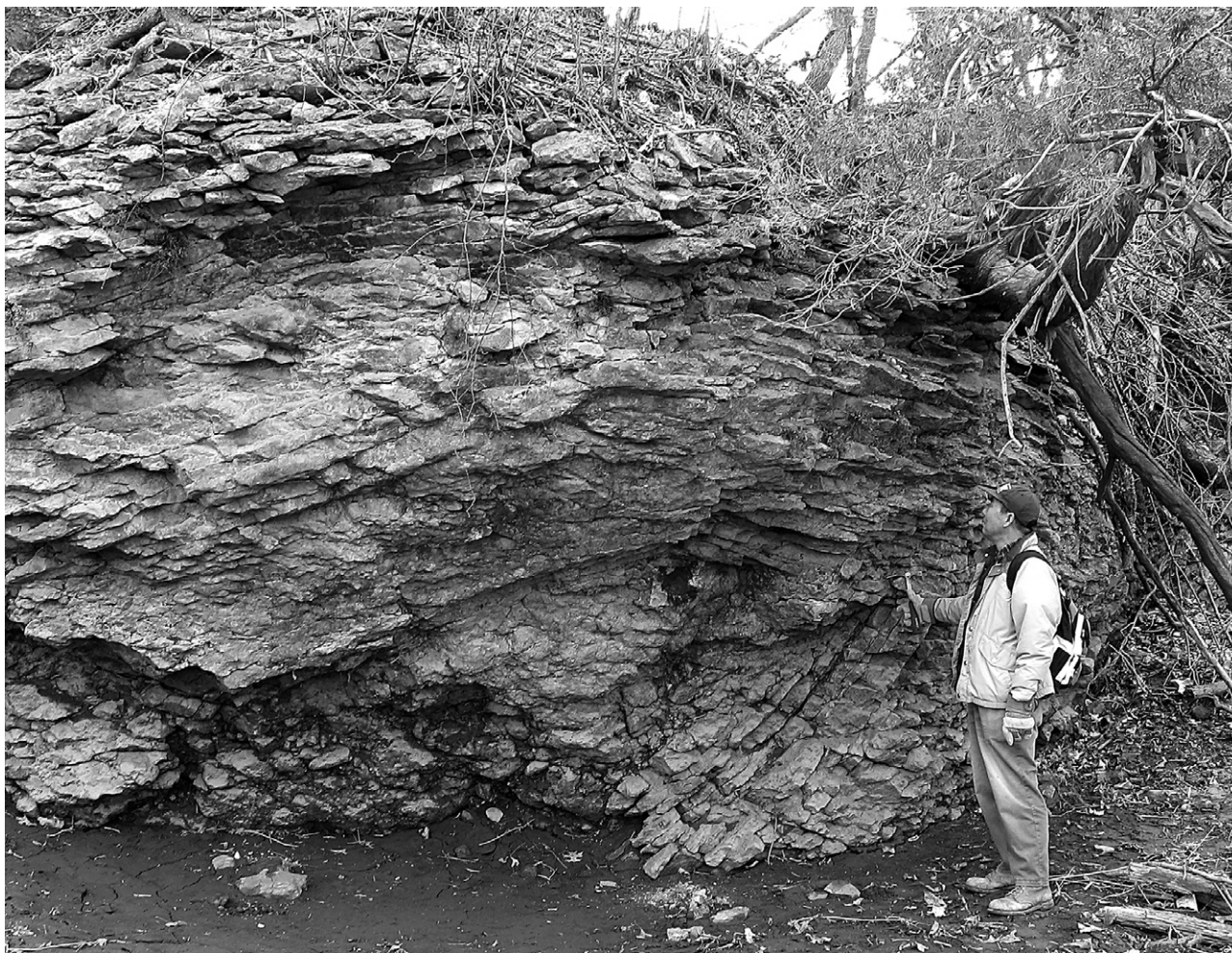


Figure 6. Macroscopic view of a segment of the H2 core (depth 33.23–33.38 m) from which sample H2-1-2 was cut at a depth of 33.36 m. The sample is a matrix-supported breccia containing larger (cm-sized) angular to subangular clasts that range in color from light gray to medium gray. These larger clasts are dominantly dolomite with lesser sandstone; white clasts are chert. The matrix is a mixture of mm- to sub-mm-sized quartz grains, lesser amounts of feldspar and glauconite grains, and dolomite grains ranging in size from silt to sand.

tails of its origin and deposition. The maximum thickness of this unit is estimated to be 184 m. This value, however, is based on cross-section constructions, which are highly dependent on only four wells with apparent full penetration of the unit (Fig. 3). In addition, only one of the full-penetration holes (Well 53572; Fig. 4) is located near the structure’s center; the others are proximal to the basin edge.

Studies of drill hole cuttings indicate that the crater-fill breccia is complex and lithologically variable (Fig. 4). Three units can be distinguished below the Winneshiek Shale in these

cuttings, particularly from Well 53572. From top to bottom, they are: (1) a series of lithologically variable breccias containing sandstone, dolomite, and minor shale (thickness ~84 m); (2) red-brown to gray-green shale (~24 m); and (3) sandstone breccia and loose sand (~52 m). The diversity of inferred rock types, and particularly the occurrence of a shale layer between



**Figure 7. Exposure of abnormally fractured and deformed Shakopee dolomite, located just outside the SE rim of the Decorah structure (see Fig. 2). View is to north; outcrop face trends approximately east-west. Mapped crater boundary is about 50 m to west (left). This outcrop, the only known surface exposure of visibly deformed pre-impact target rocks close to the structure, shows intense fracturing and deformation that are inconsistent with the typically undeformed character of the same bedrock further away from the structure. At least three sets of closely spaced subparallel fractures are visible, displaying shallow dips to the left, right, and forward (toward the observer). The V-shaped structure, immediately to the left of the geologist's right hand, may be a recumbent fold whose axial plane dips to the left. The central portion of this structure is a monomict breccia.**

two breccia units, suggests a basin-filling history that is complex and prolonged, perhaps reflecting the post-impact sedimentary complexities that occur in impact structures formed in marine targets involving a significant depth of overlying water (e.g., Ormö and Lindström, 2000; Dypvik and Jansa, 2003).

The most informative samples of the breccia unit come from partial penetrations of the upper 16–26 m of the breccia in two cores within the structure, 62035 (CS1) and 80238 (H2) (see Figs. 3 and 5); all other breccia samples are represented by drill cuttings. The breccia is composed of angular to subangular clasts of dolomite, sandstone, chert, and less shale in a matrix of very fine to coarse sand-sized dolomite and quartz, with subordinate grains of feldspar and glauconite. Clasts, in particular dolomite clasts,

range up to 25 cm in length; Figure 6 shows a representative core sample of breccia that contains smaller clasts.

In addition to the two cores, 16 logged wells yielded relatively reliable drill cuttings of sub-Winneshiek material. Prior to the recovery of the first core (H2), we suspected that several sub-Winneshiek drill cuttings sample sets represented penetration of breccia or conglomeratic strata (due to the unusual mix of rock and grain types), with occasionally observed fine matrix coating on what appeared to be small (<1 cm) clasts in a few samples. Uncertainty about the actual rock fabric prevailed, however, until we were able to directly observe the breccia fabric in core samples. This observational uncertainty must have also puzzled earlier geological survey well loggers, because historic logs, dating

between 1939 and the early 1990s, noted an abnormal mix of rock and grain types, as well as apparently abnormal formational thicknesses, even though the loggers applied normal stratigraphic calls to the logs. Upon retrieval of the two cores, which verified the presence of breccia below the shale, we reinterpreted all the historic logs and reexamined some of those sample sets. However, uncertainty concerning several aspects of both the older and more recent cuttings samples remains, most notably the exact point of contact between the crater-fill breccia and the crater wall and floor (or down-dropped blocks) in several of the wells.

Despite the inherent problems in the interpretation of drill cuttings, it is clear that the crater-fill breccia is lithologically variable horizontally as well as vertically. Examination of fragment



types in several sets of well cuttings revealed a radial cross-basin variation in the breccia unit: carbonate lithologies (dolomite) dominate near the basin rim and siliciclastic (sandstone) fragments toward the center (Fig. 8). However, the present data are not adequate to reveal whether this variation reflects processes in the primary impact (e.g., deeper excavation in the center, removing more deeply buried Cambrian sandstones) or subsequent depositional effects (heterogeneities in the source areas or sedimentary sorting mechanisms).

### Crater-Fill Units: The Winneshiek Shale

The Winneshiek Shale was originally described as “a greenish brown to dark-gray finely laminated sandy shale with a significant organic carbon and pyrite content” (Liu et al., 2006, p. 969). In outcrop and core samples, it is a series of alternating sub-mm- to mm-thick silty to sandy shale laminae suggestive of prolonged deposition in a quiet-water environment.

The Winneshiek Shale is fully penetrated by 20 drill holes and ranges in thickness from 17 to 27 m. The most reliable shale thickness data come from the two cores CS1 and H2 (62035 and 80238) and a water well (53572), which yielded a natural gamma and cuttings log (Fig. 4). Shale thickness in the cores, which are located 0.6 and 0.3 km from the basin edge and 2.2 and 2.5 km from the basin center (Figs. 3 and 18B), ranges from 17 to 18 m. Shale thickness in Well 53572, which is 0.35 km from the basin center, is 26 m as measured from consideration of both drill cuttings and a natural gamma log (Fig. 4). All subsurface and airborne electromagnetic data (Kass et al., 2013a, 2013b) suggest that the Winneshiek Shale is the uppermost basin-fill unit across the entire structure.

### SAMPLE COLLECTION, PREPARATION, AND STUDY METHODS

In typical impact structures, the diagnostic indicators of impact-produced shock metamorphism tend to be located in specific regions within the structure, particularly in units of crater-fill breccias that are deposited in the crater immediately after excavation of the original bowl-shaped cavity (see e.g., Dence, 1968; Grieve, 1987; French, 1998, Chs. 3, 5). Such units, and the shock-metamorphosed fragments they contain, have been critical in providing convincing evidence for the impact origin of suspected structures, often through samples obtained by drilling (Dence, 1968; Dence et al., 1968; Grieve, 1987). At the Decorah structure, access to these crater-fill units is severely lim-

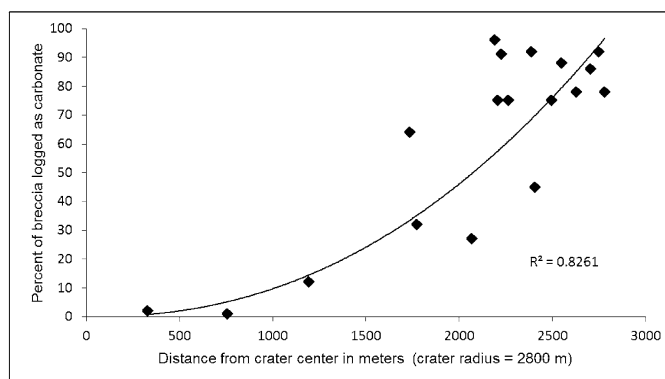


**Figure 8.** Graph showing lithologic variation of rock types in drill cuttings from the Decorah impact structure crater-fill breccias and related units as a function of radial distance within the crater. Data from 16 rotary churn-drill holes and 2 cores (e.g., Figs. 3 and 18) located at various radial distances within the structure (X-axis) are presented as the percentage of carbonate lithologies in fragments (Y-axis) as a function of distance (in m) outward from the center of the structure. The data show a pronounced change in the lithologies obtained across the crater: carbonate lithologies appear more abundant (70–100%) in the breccia units near the crater rim, while siliciclastic lithologies dominate closer to the crater center (60–90+%).

ited by the complete lack of crater-fill breccia exposures, and samples of these critical lithologies (i.e., the polymict breccias beneath the Winneshiek Shale) could be obtained only from drill holes that encountered the breccia (Figs. 3, 4, and 5).

In our study, this limitation is offset by the fact that the identification of diagnostic shock effects (especially PFs and PDFs in quartz) can be successfully carried out on small samples and even on individual mineral grains (e.g., Stöffler and Langenhorst, 1994; Grieve et al., 1996; Montanari and Koeberl, 2000). The samples studied were obtained from two drill holes on the southeast periphery of the structure that penetrated the polymict breccia underlying the Winneshiek Shale: a rotary drill hole (52450) and a shorter core-drill hole (H2). (See Fig. 18B for locations.)

Two samples, one from each hole, were selected for detailed study. (In the descriptions below, we follow earlier writers [Stöffler and Langenhorst, 1994; French et al., 2004; French and Koeberl, 2010] in using the nongenetic term *planar microstructures* [PMs] for all planar or quasi-planar deformation features in quartz, while planar fractures [PFs] and planar deformation features [PDFs] are more strictly defined and regarded as unique and diagnostic shock-wave products that identify meteorite impact events.)

1. Sample H2-1-2, a 2.5 by 4.0 cm specimen from a 5-cm-diameter drill core, comes from a depth of 33.36 m in the H2 core (Figs. 5 and

6) and was examined in a standard petrographic thin section (Fig. 9). The sample depth is ~15 m below the top of the breccia.

2. The other sample, from Well 52450, was obtained from a rotary drill hole cuttings sample composed dominantly of dolomite, single quartz grains, minor feldspar, and other minerals (Fig. 10). Sample depth was an interval of cuttings from 80.8 to 82.3 m, ~8 m below the top of the breccia unit. The quartz grains were generally loose, matrix free, and rounded to broken and angular in shape; the original content of deformed grains showing planar microdeformations (PFs and/or PDFs) was visually estimated to be ≤1% by number. This sample was washed in tap water and oven dried at 70 °C; individual grains in the range of 0.5–1.5 mm in size were then handpicked under a binocular microscope in reflected light at magnifications of less than 40×. Grains with highly developed sets of planar microstructures (PFs and PDFs) appeared white, opaque, and fractured in reflected light (Fig. 10) as a result of internal reflections. These white, opaque grains were handpicked to produce a concentrate in which the percentage of quartz grains with PFs and/or PDFs was increased from ≤1% to >75%. The concentrated grains were incorporated into an epoxy plug 2.0 cm in diameter, cemented to a thin section, and ground and polished to a standard thickness of ~0.03 mm for petrographic studies.

Petrographic thin sections from both samples were examined on a standard polarizing

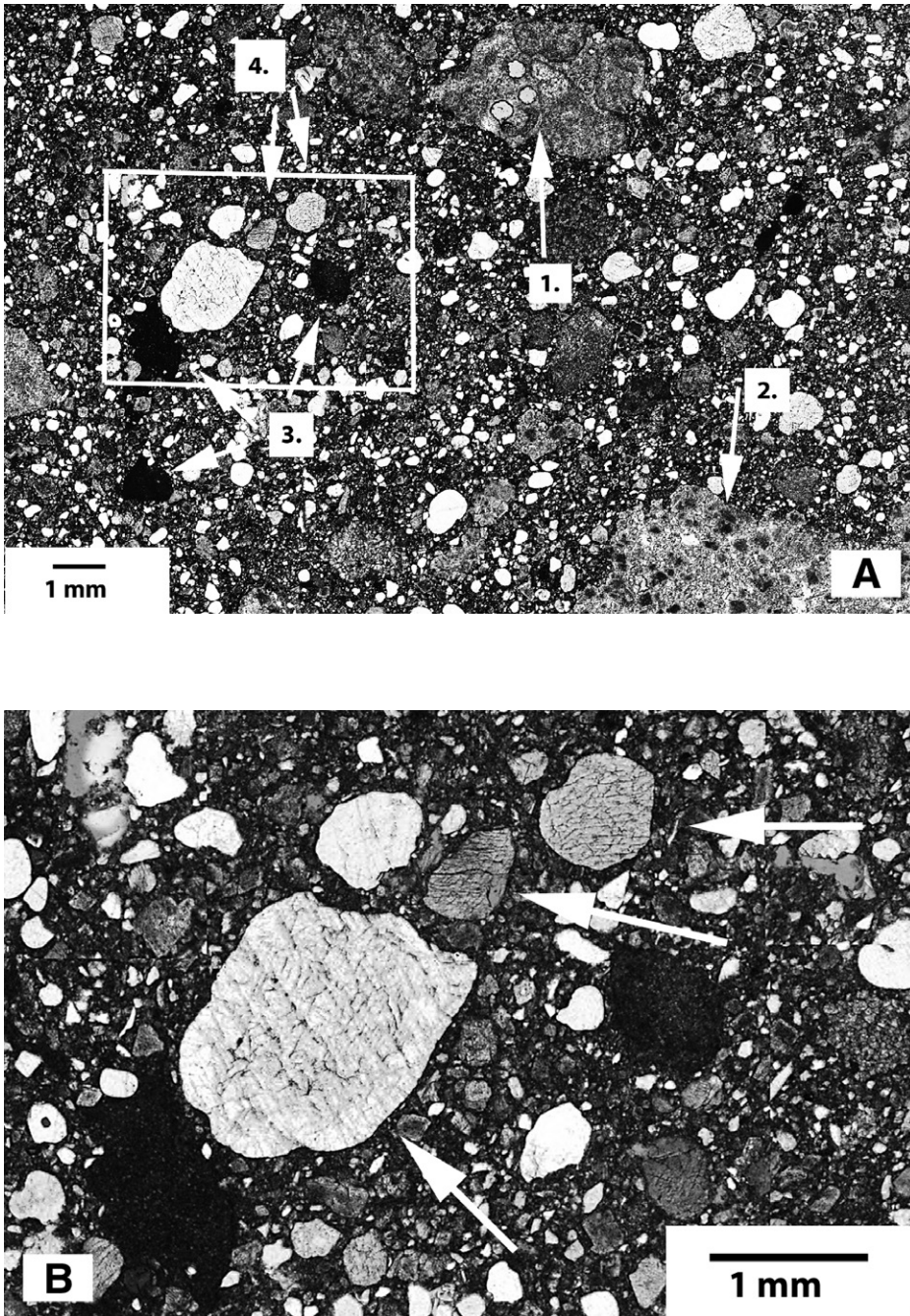
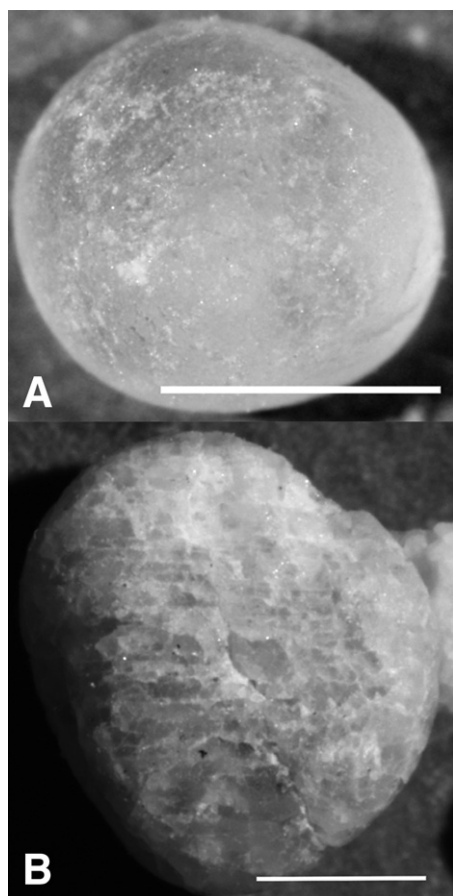


Figure 9. Microscopic views of a thin section of the breccia underlying the Winneshiak Shale in the basin of the Decorah impact structure. (Core Hole H2, Sample H2-1-2, depth 33.2–33.3 m; plane-polarized light.) (A) Wide-field view of the unit, which consists of diverse, poorly sorted rock and mineral clasts, typically a few tenths of a mm to a few cm in size, enclosed in a matrix of finer clasts and carbonate material. Gray clasts are carbonate rock fragments; smaller white clasts are individual quartz grains, usually single. The diversity of rock types in this unit includes (typical examples indicated by numbered arrows): (1) microcrystalline carbonate rock, with typical grain sizes of 50–150  $\mu\text{m}$ , containing oval structures resembling oolites or possibly microfossils (white circular areas in the clast are holes in the thin section); (2) microcrystalline carbonate rock, composed of granular carbonate (dolomite?) crystals typically 100–300  $\mu\text{m}$  in size; (3) very fine microcrystalline carbonate rock composed of crystals typically 10–50  $\mu\text{m}$  in size, accompanied by fine dark opaque material (organics?); (4) (in white-outlined box) multiple individual quartz grains containing shock-produced planar microstructures (PMs); two grains (#4, white arrows) have well-developed PMs and display a pale to dark yellowish color producing a so-called “toasted” appearance. (B) Enlarged view of area enclosed in box (inset) of (A), showing three large individual quartz grains (white arrows; center and upper center) in a matrix of small carbonate rock fragments, single quartz grains, and finer material. The three indicated quartz grains show multiple sets of PMs interpreted as shock-produced planar fractures (PFs). In contrast to the lower, larger grain (lowest arrow), which appears transparent (white) in thin section, the upper two grains (upper arrows) display a pale to dark yellowish color giving them a “toasted” appearance.



**Figure 10.** Binocular microscopic views of two quartz grain types (unshocked and shock-deformed) representative of grains found in cuttings sample from Well W52450, depth 80.8–82.3 m. Individual grains were handpicked from the sample under binocular microscope examination. (A) A typical smooth, rounded, and translucent quartz grain characteristic of the majority of quartz found in the coarser-grained Cambrian and Ordovician sandstones of the study area. Scale bar = 1 mm. (B) A white, opaque quartz grain exhibiting parallel sets of widely spaced fractures. Grains exhibiting this appearance are distinguishable from the more abundant translucent grains (A) and were concentrated by handpicking for thin sectioning and petrographic examination. Scale bar = 1 mm.

microscope (flat-stage) and then transferred to a 4-axis Leitz Universal stage (U-stage) for measurement of the *polar angles* ( $\angle c$ ) between the quartz *c*-axis and the poles to the various PF and PDF planes, using standard methods (e.g., Robertson et al., 1968; Engelhardt and Bertsch, 1969; Stöffler and Langenhorst, 1994; Grieve et al., 1996; Montanari and Koeberl,

2000, p. 295–300; French et al., 2004; Ferrière et al., 2009). Both samples provided sufficient quartz grains to produce a statistically robust number ( $> \sim 100$ ) of polar angle measurements and their angular distributions (Robertson et al., 1968; Ferrière et al., 2009). Only observable PMs were recorded; no correction was made for possible unobservable PMs lying in the “zone of inaccessibility” outside the range of possible U-stage rotations (see, e.g., Engelhardt and Bertsch, 1969; Stöffler and Langenhorst, 1994; Ferrière et al., 2009).

Polar angle measurements were initially plotted by hand to produce a standard histogram of the number of measurements versus their angular distribution (Robertson et al., 1968; Alexopoulos et al., 1988; Stöffler and Langenhorst, 1994; Grieve et al., 1996). The individual orientation measurements were then replotted on a Wulff (stereographic) stereonet with the quartz *c*-axis rotated to vertical, producing a so-called “rectified” or “spike” plot. For each measured grain, this plot was then overlain with a stereographic template of quartz orientations in order to assign specific Miller index {hkil} values to the individual planes (for details, see Engelhardt and Bertsch, 1969; Stöffler and Langenhorst, 1994; Grieve et al., 1996; Montanari and Koeberl, 2000, p. 295–300).

All plotting and {hkil} determination measurements were done by hand; although several automated methods are now available (e.g., Huber et al., 2011; Losiak et al., 2016), they have not been tested on large populations of measured PFs and PDFs, and we therefore did not apply them in this study. We used the older stereographic template (Engelhardt and Bertsch, 1969) containing 10 quartz {hkil} forms, rather than the recently proposed version containing 15 forms (introduced by Ferrière et al., 2009, Table 1). Using the older template does not result in any serious differences in the orientation patterns obtained (see discussions in Ferrière et al., 2009), and has the advantage of making it possible to compare our petrofabric results directly with those of earlier studies on other impact structures (e.g., French et al., 1974, 2004).

## RESULTS

### Sample Petrography

#### Sample H2-1-2

This sample is a fine, poorly sorted, possibly sedimentary, polymict breccia composed chiefly of a variety of fragments of carbonate and sandstone rocks and individual mineral fragments (Fig. 9A). The lithology is structureless, and individual fragments show apparently random sorting and orientation. Percentages of

different rock and mineral components (visually estimated) vary significantly with location in the thin section. Rock and mineral fragments  $\geq 1$  mm in size (and mostly as large as 5–10 mm) are typically angular and blocky and make up  $\sim 50\%$  of the sample. Most of these fragments consist of various microcrystalline carbonate lithologies with grain sizes ranging from fine- (50–100  $\mu\text{m}$ ) to medium-grained (0.1–0.4 mm). All the carbonate appears to be dolomite, with no calcite present. Some carbonate fragments contain occasional thin layers of small (0.1–0.5 mm) rounded quartz grains. A few typical carbonate fabrics, such as oolitic to peloidal, are evident in the dolomite clasts; such textures are found in both the Oneota and Shakopee formations.

Single quartz grains 0.2–2 mm in size constitute  $\sim 25\%$  of any given field of view, and a few exotic grains and fragments are present: microcrystalline chert, shale, crystalline quartz-rich and quartz-feldspar metamorphic(?) rocks, and fine-grained quartz-feldspar (volcanic?) rocks with lath-like feldspars forming apparently microgranophytic textures. The single mineral grains are overwhelmingly quartz, with very rare feldspar and glauconite. The feldspar grains are fine- to very fine-grained and usually have a rounded grain core with angular feldspar overgrowths, a texture typical for very fine- to fine-grained feldspathic sandstones in the Upper Cambrian of the Mississippi Valley region (Odom, 1975). Matrix materials (rock and mineral fragments  $< 1$  mm), including single quartz grains, constitute  $\sim 50\%$  of the unit, and the individual rock and mineral fragments ( $\geq 1$  mm), chiefly carbonate rocks, chert and individual quartz grains, occur in a fine microcrystalline carbonate cement ( $\sim 5\%$ ).

The breccia consists almost entirely of rock and mineral fragments derived from local sandstone and carbonate strata that enclose the Decorah structure, together with a small percentage of granitic and volcanic(?) lithologies probably derived originally from the underlying Precambrian crystalline basement. The rarity of these latter fragments ( $\leq 1\%$ ) in the breccia suggests that they were not derived from direct excavation of the basement but were present as isolated pre-impact clasts in the younger sediments (e.g., the Cambrian sandstones) that were excavated by the impact (see Table 1).

Individual quartz grains constitute  $\sim 25\%$ – $50\%$  of the matrix material and up to 25% of the overall sample, although estimated percentages vary significantly (from 10 to 25%) with location in the thin section. The quartz grains are generally single individuals, spheroidal to ellipsoidal in shape, and generally rounded to subrounded (Fig. 9B), although small grains

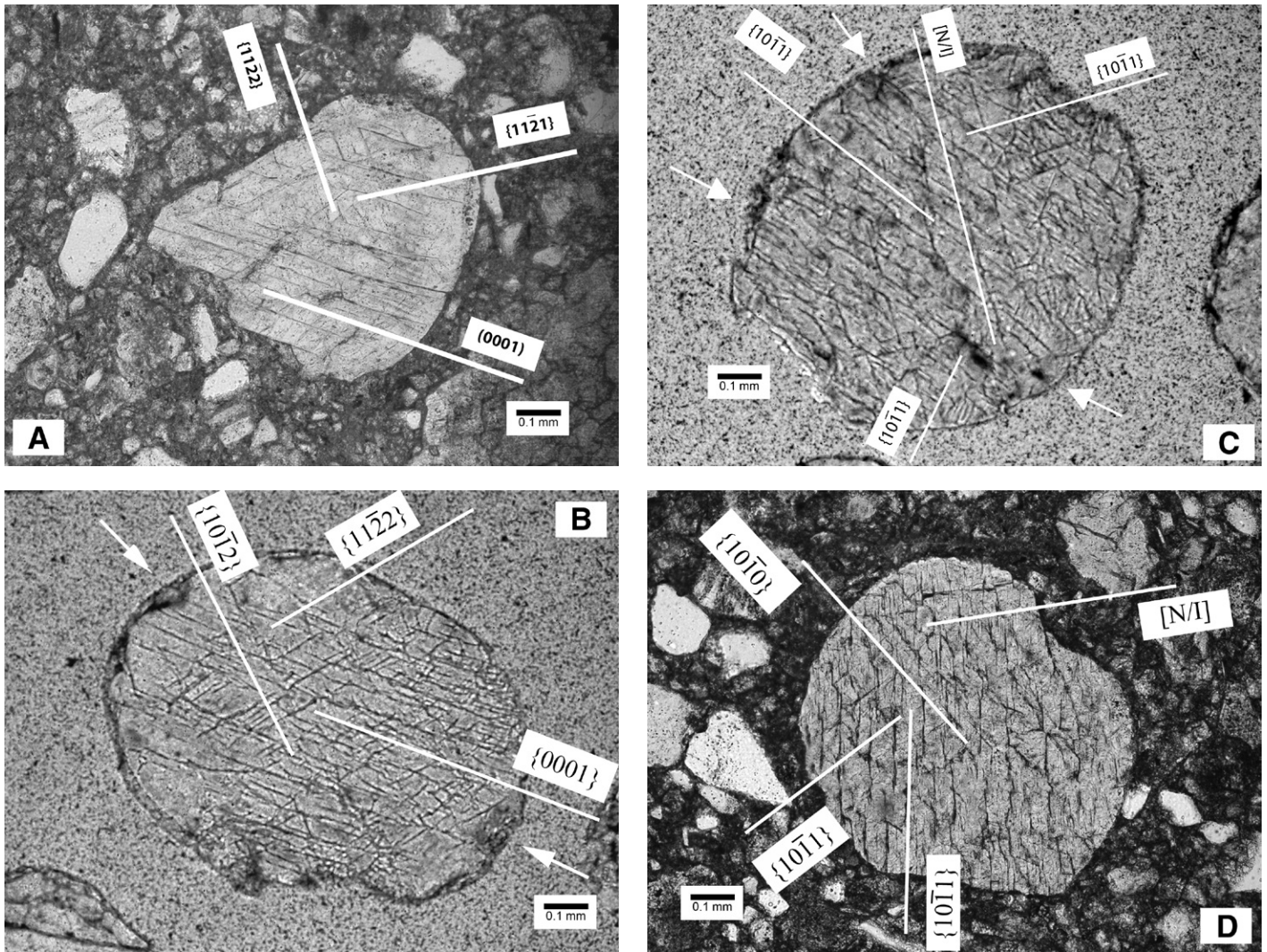


Figure 11. Shock-produced planar microstructures (“P1 features” or planar fractures [PFs]), developed in individual quartz grains from crater-fill breccia unit of the Decorah impact structure. (A) Irregular, partly rounded individual quartz grain from the breccia unit underlying the Winneshiek Shale, showing three sets of shock-produced PFs: a prominent set parallel to the base (0001) and subordinate sets parallel to the  $\{11\bar{2}1\}$  and  $\{11\bar{2}2\}$  planes. The lower boundary of the grain shows a steplike character produced by the spalling of quartz fragments along the fracture sets, indicating that the separation planes are indeed open fractures. (Core Hole H2, Sample H2-1-2, depth ~33.2–33.3 m; Grain #4,1; plane-polarized light.) (B) Well-rounded single quartz grain showing three well-developed sets of shock-produced PFs parallel to the base (0001) and to the  $\{11\bar{2}2\}$  and  $\{10\bar{1}2\}$  planes. Small darker patches along the grain margin (white arrows) are actually small areas where P2 features (planar deformation features [PDFs]) are developed. (From sorted grain mount prepared from drill cuttings, Well “Leon Steinlage” W-52450, depth ~80.8–82.3 m; Grain #11,1; plane-polarized light.) (C) Well-rounded single quartz grain showing three sets of shock-produced PFs parallel to distinct  $\{10\bar{1}1\}$  planes in the crystal. (A fourth set of apparent PFs is also observed but could not be indexed [“N/I” = not indexed]). Small, slightly darker, patches along the grain margin (arrows) are actually small areas where P2 features (PDFs) are locally developed. (From sorted grain mount prepared from drill cuttings, Hole “Leon Steinlage” W-52450, depth ~80.8–82.3 m; Grain #20,1; plane-polarized light.) (D) Large well-rounded quartz grain, with a partly angular rim, from the crater-fill breccia unit underlying the Winneshiek Shale. The grain shows three sets of well-developed shock-produced PFs parallel to the  $\{10\bar{1}0\}$  and  $\{10\bar{1}1\}$  planes; a fourth set of possible PFs (“[N/I]”) could not be indexed. (Core Hole H2, Sample H2-1-2, depth 33.2–33.3 m; Grain #227,1; plane-polarized light.)



(<0.1 mm) may be angular, possibly because they are fragments derived from larger grains. These quartz grains could be sourced from any quartzose sandstone units in the sedimentary section, e.g., the Ordovician basal Shakopee, or the Cambrian Jordan formations (see Table 1). If the impact process excavated sedimentary rock units deeper than the Lone Rock, the coarser quartz grains could also have been derived from the Wonewoc or Mt. Simon formations.

#### Sample W-52450

The handpicked quartz grains in this sample are typically 0.5–1.5 mm in size, spheroidal to ellipsoidal in shape, and well-rounded to sub-rounded. Out of 96 total grains, 93 were quartz and 3 were carbonate. Out of the 93 quartz grains, 73 (78%) contained measurable sets of planar microstructures (both PFs and PDFs). The remaining 20 quartz grains were not measurable for several reasons: extreme marginal cracking during preparation (16), polycrystallinity and small individual grain sizes (3), and apparent absence of any planar microstructures (1).

#### Deformation of Quartz Grains

In the thin section of sample H2-1-2, the majority of quartz grains show no unusual deformation and display only features characteristic of normal metamorphism (for descriptions, see, e.g., Spry, 1969; Vernon, 2004; French and Koeberl, 2010, and references therein). Most of the quartz grains are undeformed or only slightly deformed; extinction under crossed polarizers is generally sharp (<5°), occasionally slightly undulose (5–10°), and rarely strongly undulose (>10°). In rare cases, deformation bands or segmented extinction in adjacent areas are evident, but no multiple small domains (“mosaic extinction”) were observed. Typical metamorphic deformation lamellae (Böhm lamellae or MDLs) were observed in only a few grains. The sample of rotary cuttings (sample W-52450) is similar; most of the individual quartz grains show similar features and lack any unusual deformation effects.

Significant percentages of quartz grains in both samples show single or multiple parallel sets of planar microstructures (PMs) in various orientations. Such features occur in ≤1% of the grains in sample H2-1-2 (Fig. 9B) and >75% of the individual handpicked grains from sample W-52450. The observed PMs are of several different types; some represent the results of normal crystallization and metamorphism; others are due to shock deformation (for discussions, see, e.g., French and Koeberl, 2010, p. 133–141). For convenience in detection, measurement, data reduction, and interpretation, we first classify PMs into two nongenetic categories, P1

and P2, an informal terminology used in studying similar shocked sedimentary rocks from the Rock Elm structure, Wisconsin (French et al., 2004). P1 features are larger, darker, more widely spaced, and more continuous across a larger fraction (typically >50%) of an individual grain; they are interpreted as shock-produced open fractures (cleavage), identical to the features designated as planar fractures (PFs) (Stöffler and Langenhorst, 1994). P2 features designate shorter, narrower, and more closely spaced closed structures that may have a variety of characteristics and origins: healed fractures, subsidiary fractures in *feather-fracture features* (French et al., 2004; Poelchau and Kenkmann, 2011), and genuine shock-produced planar deformation features (PDFs) (Stöffler and Langenhorst, 1994; Grieve et al., 1996).

#### P1 Features

P1 features (or PFs) are the dominant PMs observed in shocked quartz grains from the Decorah structure (Fig. 11). They form multiple sets of diversely oriented planes within single host quartz grains, and they occur in virtually all grains that show any shock-produced PMs. Typically, 1–5 distinct sets of P1 planes are present in individual grains, and larger numbers (≤8) are occasionally present. In both Decorah

samples, most grains with P1 features exhibit 2, 3, or 4 distinct sets. Values for sample H2-1-2 are: 2 (25%), 3 (36%), and 4 (11%). Individual P1 planes are generally dark, uniformly planar, between 1 and 2.5 μm thick, and spaced at distances of 10–25 μm. Mutual offsets along intersecting sets of planes have not been observed. Fracturing and spalling of the host quartz grains has occasionally occurred along the planes of P1 features, forming sharp, step-like grain boundaries in which the “steps” are continuous with, or parallel to, specific P1 features in the grain (Fig. 12). Within other grains, the development of small rhombic blocks, parallel to existing P1 features, is evident. These observations indicate that the P1 features are themselves discrete open fractures within the quartz grain, along which subgrain fragments have easily separated. The dark color of individual P1 planes may be produced by a filling of exotic material (e.g., clay minerals) within the fractures, although no specific birefringent materials were observed (see French et al., 2004, p. 205).

#### P2 Features

P2 features in Decorah quartz grains are generally light-colored and form small, isolated areas typically ≤100 μm in size, commonly located at the corners, or along the edges, of

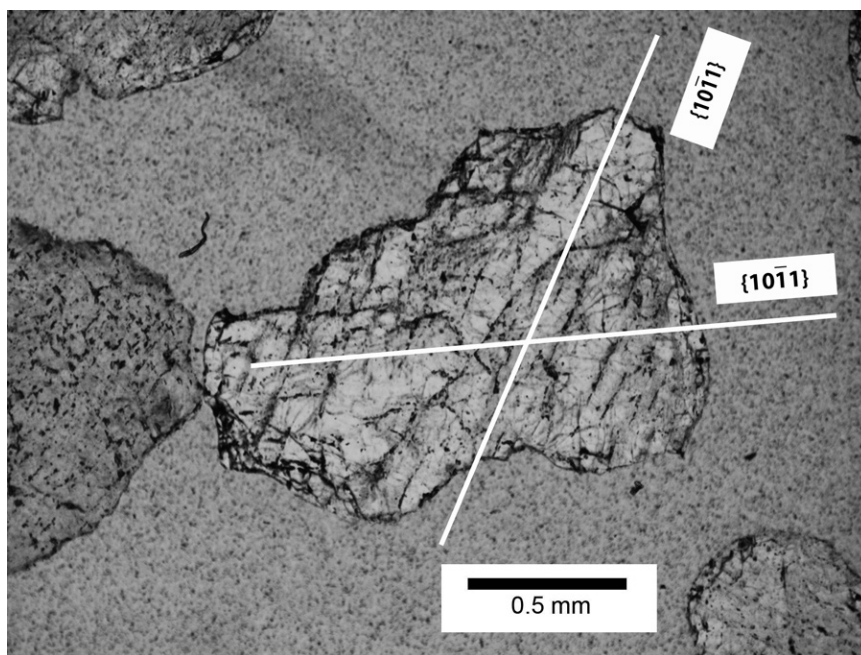


**Figure 12.** Irregular quartz grain showing two poorly developed sets of shock-produced planar fractures (PFs) parallel to  $\{10\bar{1}1\}$ . The upper edge of the grain shows a pronounced steplike boundary produced by spallation of the marginal parts of the quartz grain along the PFs (see also Fig. 11A). (From sorted grain mount prepared from drill cuttings, Hole “Leon Steinlage” W-52450, depth ~80.8–82.3 m; Grain #32,1; plane-polarized light.)



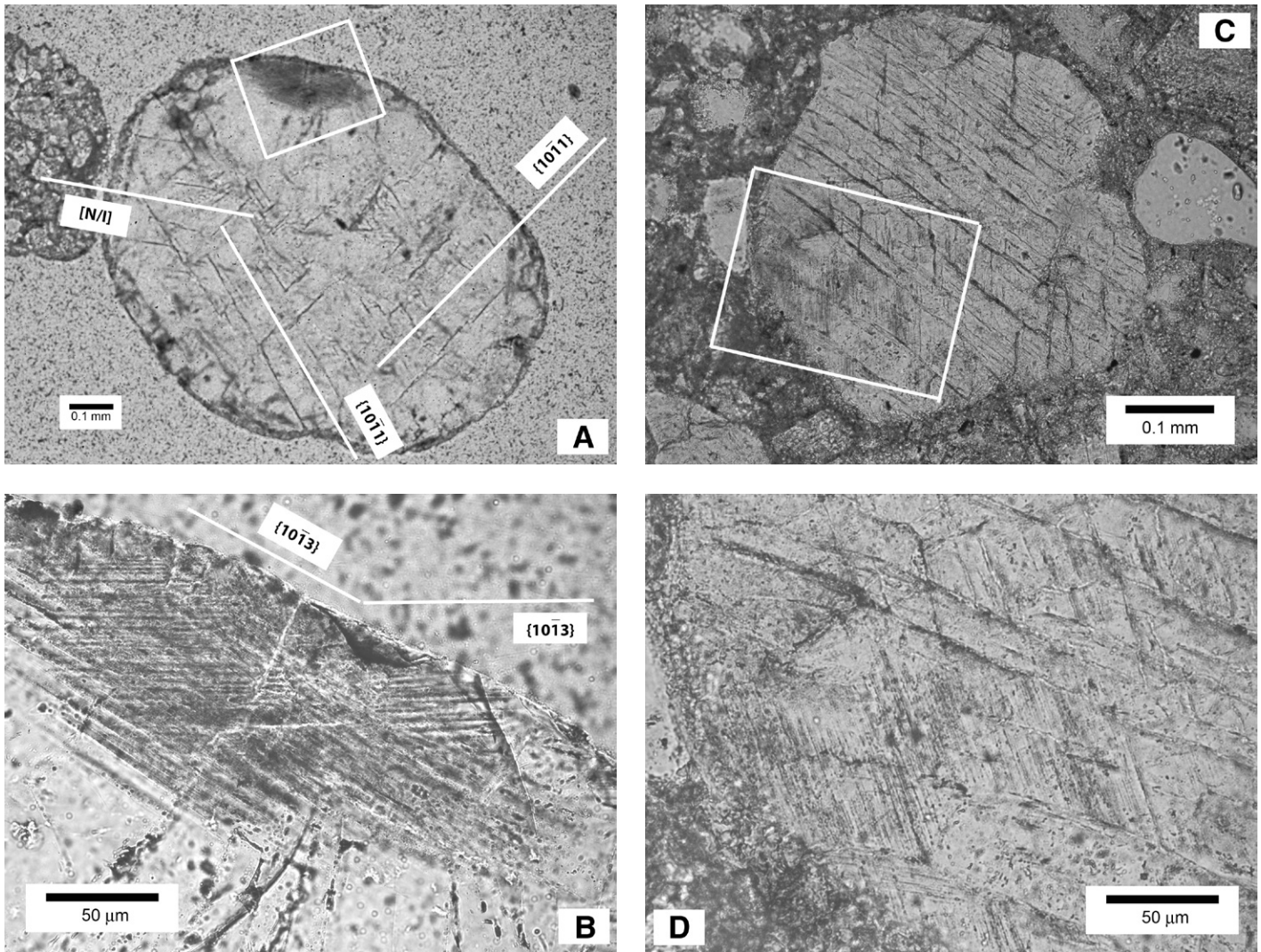


Figure 13. (A) Well-rounded quartz grain showing two sets of shock-produced planar fractures (PFs) parallel to  $\{10\bar{1}1\}$  and a third unindexed set of less developed PFs ( $[N/I]$ ). Darker marginal patch at the top of grain (white box) is a small area where P2 Features (planar deformation features [PDFs]) are locally developed (see Fig. 13B). (From sorted grain mount prepared from drill cuttings, Hole “Leon Steinlage” W-52450, depth ~80.8–82.3 m; Grain #64,1; plane-polarized light.) (B) Enlarged view of area shown in Figure 13A, showing details of darker patch along grain margin. Dark area is seen to be composed of two intersecting sets of thin, optically distinct, sets of P2 features (PDFs), oriented parallel to the distinctive, shock-produced  $\omega\{10\bar{1}3\}$  direction. (From sorted grain mount prepared from drill cuttings, Hole “Leon Steinlage” W-52450, depth ~80.8–82.3 m; Grain #64,2; plane-polarized light.) (C) Partly rounded to angular quartz grain from the crater-fill breccia unit underlying the Winneshiek Shale, showing good development of two sets of shock-produced P1 Features (PFs) (N-S and NW-SE orientations in photo; actual orientations could not be determined because the grain was not accessible on the U-stage.) In the lower left area of the grain (white outline box and Fig. 13D) P2 features (PDFs) are extensively developed in the areas between the PFs. (Core Hole H2, Sample H2-1-2, depth ~33.2–33.3 m; Grain #155,1; plane-polarized light.) (D) Enlarged view of area of grain (box) shown in Figure 13C. Parallel PFs trend WNW–ESE. PDFs, which trend NNW–SSE and appear as shorter, closely spaced narrow planes in the quartz between the PFs (especially at the lower left center of the picture), show the close spacing and optically distinct appearance from the host quartz that is typical for PDFs. (Actual orientations could not be determined because the grain was not accessible on the U-stage.) (Core Hole H2, Sample H2-1-2, depth ~33.2–33.3 m; Grain #155,2; plane-polarized light.)

quartz grains, and more rarely within the grains themselves (Fig. 13). Where present, P2 features generally form multiple sets, typically 2–4 per grain. Individual planes are sharply planar, clear, closely spaced, and locally continuous, and their visibility appears to be enhanced by refractive-index differences (“Becke line effects”) between the planes and the host quartz. The close spacing and optical effects associated with P2 features make measurements difficult, but typical widths appear to be 0.5–1  $\mu\text{m}$ , with spacings of 1.5–2  $\mu\text{m}$ . In the handpicked grains from sample W-52450, P2 features occur in ~60% of the 77 measured grains that also show P1 features. In both samples, P2 features were found alone in only one quartz grain.

The characteristics of P2 features in the Decorah samples (multiplicity, narrowness, close spacing, and possible refractive index effects) are virtually identical to those of shock-produced PDFs (e.g., Alexopoulos et al., 1988; Stöffler and Langenhorst, 1994; Grieve et al., 1996; Ferrière et al., 2009), and the orientation patterns obtained from U-stage measurements (described below) support that interpretation. The Decorah P2 features differ from those in deformed quartz from the Rock Elm structure, Wisconsin (French et al., 2004), where P2 features are typically short, planar to subplanar, and inclusion-decorated, resembling healed fractures. The Rock Elm P2 features are commonly

associated with P1 features (planar fractures) forming distinctive feather features that have been suggested as diagnostic for low-pressure shock waves in impact structures (French et al., 2004; Poelchau and Kenkmann, 2011). Although feather features are common in the Rock Elm rocks (French et al., 2004), they were only rarely observed in quartz grains from our Decorah samples (for an example, see Fig. 14), where individual sets of both P1 and P2 features are the most common deformation features.

In contrast to the mild deformation observed in the majority of quartz grains from our Decorah samples (see above), grains containing P1 and P2 features are significantly deformed themselves. In cross-polarized light, extinction is highly undulose to irregular, often forming a variable mosaic pattern. Such extreme deformation and extinction effects appear restricted to grains that display obvious P1 and P2 features. Rare quartz grains with P1 and P2 features also show a pale-yellow to medium yellow-brown color (“toasting”) in transmitted light in thin section, an effect attributed (Whitehead et al., 2002) to the presence of small fluid inclusions associated with shock-produced PDFs. This “toasting” effect is observed only in a small fraction of grains with P1 and P2 features. The grain darkening produced by the presence of P1 features, combined with the color effects of “toasting” (where present), allow these shock-

deformed grains to be quickly distinguished in thin section from the more abundant clear and undeformed grains (Figs. 9A and 9B).

### Orientation Patterns of Planar Microstructures (P1 and P2 Features)

The measurement of planar microstructure (PM) orientations in quartz-bearing samples from suspected impact structures, and the demonstration that such orientations are uniquely different from those produced by non-impact processes, have been critical to the recognition of terrestrial impact structures for several decades (see papers in French and Short, 1968; Stöffler and Langenhorst, 1994; Grieve et al., 1996; Ferrière et al., 2009; French and Koeberl, 2010).

To obtain PM orientation data for the Decorah structure, we measured suites of quartz grains containing >100 PMs in both of our Decorah samples (sample H2-1-2: 122 planes/28 grains and sample W-52450: 376 planes/77 grains) (Table 2). Histogram plots of frequency versus polar angle were constructed separately for P1 features, P2 features, and total (P1 + P2) features (Figs. 15A, 15C, and 15E, and 16A, 16C, and 16E). In addition, rectified (“spike”) plots were determined for the same populations (Figs. 15B, 15D, and 15F, and 16B, 16D, and 16F).

P1 features (PFs) are well expressed in quartz grains in both samples, with multiple sets ob-

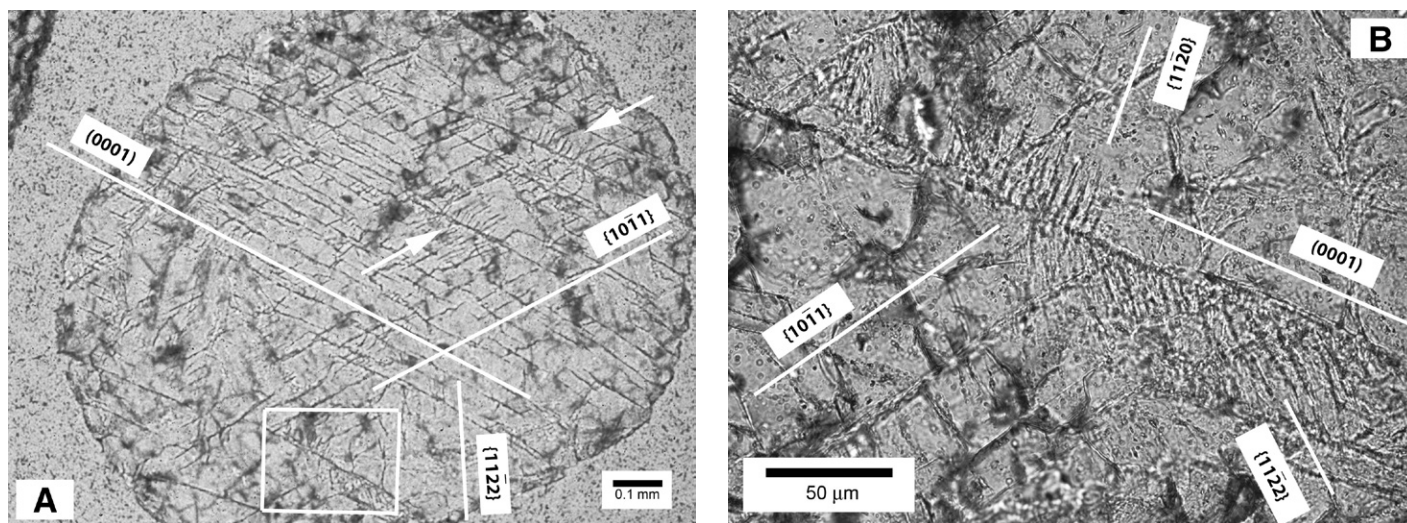


**Figure 14.** (A) Highly rounded elliptical quartz grain showing three sets of planar fractures (PFs) parallel to the (0001),  $\{10\bar{1}1\}$ , and  $\{11\bar{2}2\}$  planes. A few of the individual fractures show, e.g., in upper right and lower center parts of the grain (white arrows and white outline box), the development of distinctive feather features, in which short parallel planar microstructures (PMs) develop at an angle to the fracture with one end based on the fracture itself. (See enlarged view [inset, white outline box] in Fig. 14B.) (From sorted grain mount prepared from drill cuttings, Hole “Leon Steinlage” W-52450, depth ~80.8–82.3 m; Grain #88,1; plane-polarized light.) (B) Enlarged view of area shown in box in Figure 14A, showing development of short, closely spaced feather features along longer, more widely spaced planar fractures (PFs) parallel to the (0001) and  $\{10\bar{1}1\}$  planes. The shorter, more closely spaced feather features themselves are oriented parallel to the  $\{11\bar{2}0\}$  and  $\{11\bar{2}2\}$  planes. (From sorted grain mount prepared from drill cuttings, Hole “Leon Steinlage” W-52450, depth ~80.8–82.3 m; Grain #88-2, plane-polarized light.)

TABLE 2. PLANAR MICRODEFORMATION FEATURES IN QUARTZ: DECORAH STRUCTURE, IOWA

Symbol*	{hkil} <sup>†</sup> values	Polar angle (°)	P1		P2		P1 + P2	
			no.	(%)	no.	(%)	no.	(%)
<b>Sample H2-1-2 (Core Sample)</b>								
c	{0001}	0.0	11	15	3	6	14	11
ω	{10 $\bar{1}$ 3}	23.0	4	6	5	10	9	7
π	{10 $\bar{1}$ 2}	32.4	1	1	3	6	4	3
ξ	{11 $\bar{2}$ 2}	47.7	10	14	6	12	16	13
r/z	{10 $\bar{1}$ 1}	51.7	16	23	8	16	24	20
s	{11 $\bar{2}$ 1}	65.6	3	4	4	8	7	6
ρ	{21 $\bar{3}$ 1}	73.7	4	6	1	2	5	4
x	{51 $\bar{6}$ 1}	82.0	5	7	2	4	7	6
m	{10 $\bar{1}$ 0}	90.0	1	1	5	10	6	5
a	{11 $\bar{2}$ 0}	90.0	0	0	0	0	0	0
Not Indexed			16	23	14	27	30	25
Total			71	100	51	101	122	100
No. of Planes (P)			71		51		122	
No. of Grains (G)			28		28		28	
P/G ratio			2.5		1.8		4.4	
<b>Sample W-52450 (Grain Mount), Total Planar Microstructures</b>								
c	{0001}	0.0	41	15	9	9	50	13
ω	{10 $\bar{1}$ 3}	23.0	7	3	13	13	20	5
π	{10 $\bar{1}$ 2}	32.4	8	3	6	6	14	4
ξ	{11 $\bar{2}$ 2}	47.7	33	12	8	8	41	11
r/z	{10 $\bar{1}$ 1}	51.7	106	39	18	17	124	33
s	{11 $\bar{2}$ 1}	65.6	7	3	4	4	11	3
ρ	{21 $\bar{3}$ 1}	73.7	13	5	3	3	16	4
x	{51 $\bar{6}$ 1}	82.0	12	4	8	8	20	5
m	{10 $\bar{1}$ 0}	90.0	12	4	8	8	20	5
a	{11 $\bar{2}$ 0}	90.0	0	0	0	0	0	0
Not Indexed			33	12	27	26	60	16
Total			272	100	104	102	376	99
No. of Planes (P)			272		104		376	
No. of Grains (G)			77		77		77	
P/G ratio			3.5		1.4		4.9	

Note: Samples are stored in the collections of the Iowa Geological Survey, IHR—Hydroscience & Engineering, University of Iowa, Iowa City, Iowa, 52242.  
\*Crystallographic plane.  
†Miller-Bravais Index.

served in  $\leq 1\%$  of the grains in a given sample. The P1 orientations show fabrics typical for PFs in shocked sedimentary rocks at numerous impact structures (French et al., 1974, 2004; Grieve et al., 1996). This pattern is characterized by strong concentrations of planes parallel to the polar angles of  $0^\circ$ ,  $48^\circ$ – $52^\circ$ , and  $90^\circ$ , corresponding to the planes c{0001},  $\xi\{11\bar{2}2\}$ , (r,z){10 $\bar{1}$ 1}, and a{11 $\bar{2}$ 0} (Figs. 15A, 15B, 16A, and 16B). The three largest peaks of the measured P1 features in W-52450 correspond to the planes (r,z){10 $\bar{1}$ 1} (39%), c{0001} (15%), and  $\xi\{11\bar{2}2\}$  (12%). The “not indexed” (N/I) values for the different populations in both samples H2-1-2 and W-52450 (11%–23%) are comparable to those measured from established impact structures ( $\leq 10\%$ – $20\%$ ; Grieve et al., 1996; Ferrière et al., 2009).

P2 features in the Decorah samples are interpreted as definite PDFs (see above). Their

orientations patterns (Figs. 15C, 15D, 16C, and 16D) show significant peaks at polar angles of  $0^\circ$ ,  $48^\circ$ ,  $52^\circ$ , and  $90^\circ$ , similar to those shown by the P1 features (see above). In addition, the P2 orientations show significant peaks at angles of  $23^\circ$  and  $32^\circ$ , corresponding to the well-known  $\omega\{10\bar{1}3\}$  and  $\pi\{10\bar{1}2\}$  planes that are typical of shock-metamorphosed crystalline rocks (Robertson et al., 1968; Grieve et al., 1996). The P2 orientations in Decorah samples show more and smaller peaks than those for the P1 planes. The three largest peaks for all P2 samples in W-52450 correspond to (r,z){10 $\bar{1}$ 1} (17%),  $\omega\{10\bar{1}3\}$  (13%), and c{0001} (9%). The significant presence of orientations parallel to  $\omega\{10\bar{1}3\}$  and  $\pi\{10\bar{1}2\}$  is consistent with the interpretation of P2 features as PDFs.

In the Decorah samples, both P1 and P2 features show strong concentrations at specific

polar angles, particularly  $\sim 0^\circ$ ,  $\sim 50^\circ$ , and  $\sim 90^\circ$ . Such concentrations are typical for the fabrics produced by shock metamorphism, and the Decorah plots are closely similar to plots from two other established impact structures: the BP site, Libya (French et al., 1974) and Rock Elm, Wisconsin (French et al., 2004) (Fig. 17).

The “not indexed” values for P2 features (21%–35%) are higher than those for P1 features (11%–23%). This situation may reflect a lower degree of measurement precision, which would in turn produce a lower precision of {hkil} assignments. Possible explanations include: (1) the designation as P2 features of multiple features with different origins, e.g., true PDFs, rarer feather-fracture features, and other small unidentified deformations; (2) the difficulty of measuring even true PDFs because of their generally vague, restricted, and patchy character in the quartz grains studied.

Despite these difficulties, orientation fabrics for the Decorah samples (Figs. 15, 16, and 17) are closely comparable to those determined for shocked quartz at established impact structures, and the data presented here constitute solid evidence for the action of shock waves on these samples and, therefore, for the origin of the Decorah structure by meteorite impact.

## DISCUSSION

### Planar Microstructures: Orientation Diagrams, Statistical Evaluation, and Occurrence

#### Use of Traditional Plotting and Data-Reduction Methods

Until recently, PM orientation diagrams have been plotted and evaluated by hand, and the use of such plots to identify shock environments and meteorite impact structures has been done largely by inspection and qualitative comparison, relying on: (1) the uniqueness of shock-produced orientation fabrics; (2) their similarities to orientation patterns from experimentally shocked samples or from established impact structures; and (3) the clear differences between the orientations of shock-produced PMs and those produced by non-shock geological processes (see, e.g., French and Short, 1968; Engelhardt and Bertsch, 1969; Alexopoulos et al., 1988; Stöffler and Langenhorst, 1994; Grieve et al., 1996; Ferrière et al., 2009; French and Koeberl, 2010). More recently, attempts have been made to develop rapid and accurate computerized methods to replace the hand-plotting of orientation histograms and the use of a hand-manipulated stereonet to determine the {hkil} values of individual PM sets (Huber et al., 2011; Losiak et al., 2016). At the same time, a related

Decorah, IA. Core Sample H2-1-2 (Quartz microbreccia) Thin Section, Grain Numbers 201-228

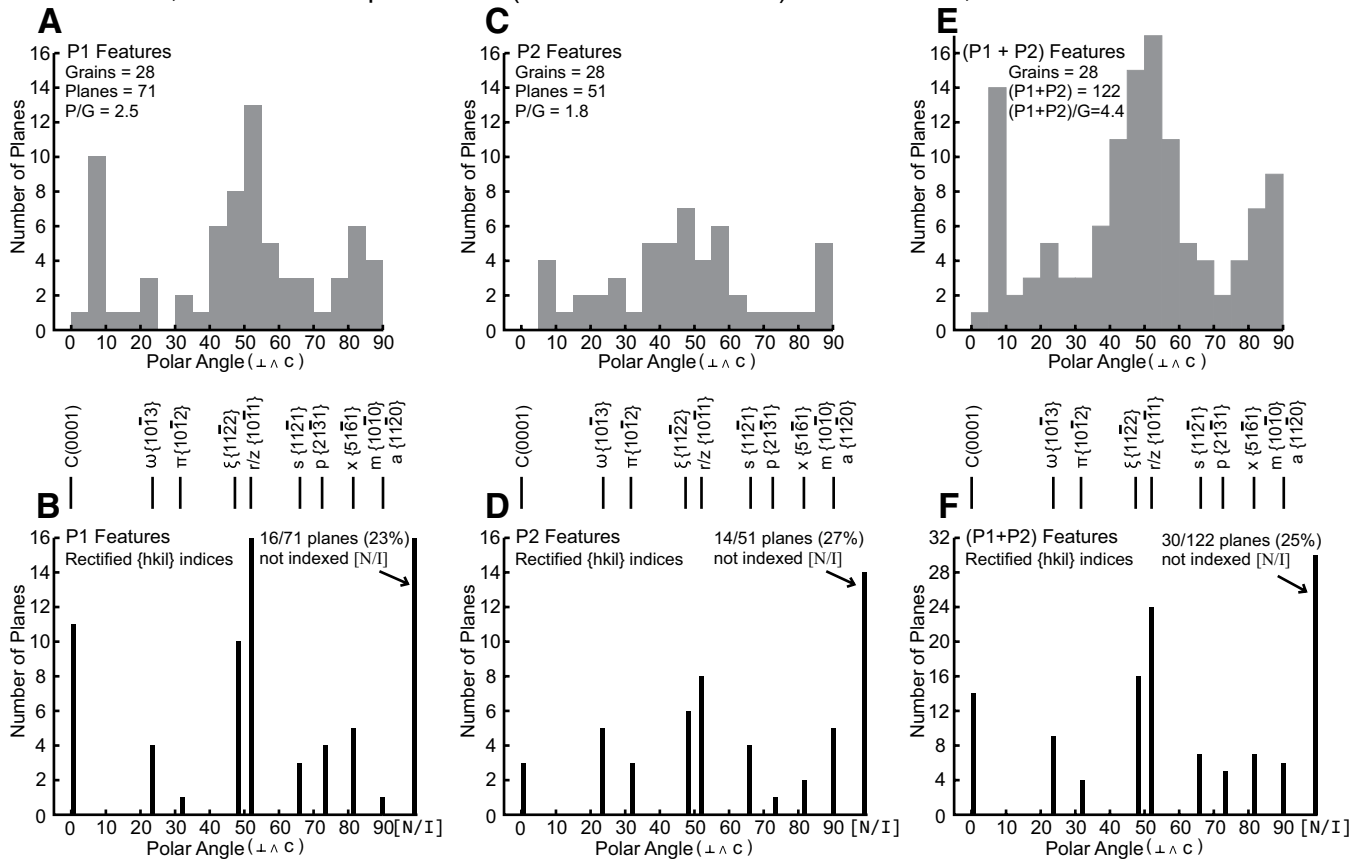


**Figure 15.** Graphs of orientations of planar microstructures in quartz grains from crater-fill breccia unit filling the Decorah structure (Sample H2-1-2; depth interval 33.2–33.3 m; see Fig. 9). Histogram plots show frequencies of different angles between quartz *c*-axis and pole to plane for P1 features (cleavage, fractures: A, B), P2 features (possible planar deformation features [PDFs] and other features: C, D), and total features (P1 + P2) (E, F). Two types of histograms are shown: (1) unmodified frequency data for polar angles (A, C, E), and (2) “rectified” or “spike” plots (B, D, F) derived from a *c*-axis-vertical orientation and allowing identification of {hkil} Miller index values for specific planes (for details, see Grieve et al., 1996; Ferrière et al., 2009). Note, in both types of plots, the strong concentrations of planes corresponding to specific orientations, e.g., (0001) (0°), {10 $\bar{1}$ 3} (23°), {11 $\bar{2}$ 2} (48°), and {10 $\bar{1}$ 1} (52°). Such concentrations are typical and diagnostic for shock-produced deformation features in quartz grains from established impact structures.

development has been the design and use of a new stereonet template containing 15 {hkil} forms (Ferrière et al., 2009) to replace the traditional and established version (Engelhardt and Bertsch, 1969) containing only 10 forms.

Computerized data-reduction for PM orientation measurements is a highly desirable goal; such methods would produce major savings in time, significant improvements in overall accuracy and confidence, and the ability to measure and process more and larger batches of PM orientation data in shorter periods of time. However, in this paper, we have used the established methods (hand-plotting and the 10-form stereonet) for the Decorah samples for several reasons beyond the obvious ones of convenience and familiarity: (1) the computer methods have not yet been tested and evaluated by comparing large batches of real data on both known and

suspect impact structures, and it is possible that significant modifications may still be required; and (2) the old-style orientations can be compared directly, both visually or with simple statistical analysis, with similar plots determined for impact structures over several decades (Grieve et al., 1996) (see Fig. 17).

Detailed statistical comparisons between the “old” and “new” methods of PM plotting and evaluation have yet to be made, but it is unlikely that our use of the “old” system will compromise our conclusions. The five new {hkil} forms in the “new” stereonet (Ferrière et al., 2009) involve only a small percentage of the planes measured in a typical sample; for example, only a small fraction of  $\omega\{10\bar{1}3\}$  planes in the “old” system would be shifted to the “new” {10 $\bar{1}$ 4} plane (see Ferrière et al., 2009, p. 934), and this is unlikely to result in major differences in {hkil}

assignments between the “old” and “new” stereonets. Orientation diagrams will appear similar regardless of which stereonet is used, and the identifying characteristics of shock-produced orientations, i.e., extreme concentrations at specific {hkil} planes, will be evident in either stereonet. If more planes can be indexed with the “new” stereonet, the percentage of “not indexed” (“N/I”) planes will be reduced (Ferrière et al., 2009, p. 934). Until the “old” and “new” plotting systems are rigorously compared, however, there is no objective basis for determining which one is a more reliable indicator of shock-produced PM orientation fabrics in samples from suspected impact structures.

**Ambiguities in {hkil} Assignments**

A significant, although not serious, problem with either system of plotting and data reduc-

Decorah, IA. Sample W-52450 grain mount, Grain Numbers 3-93

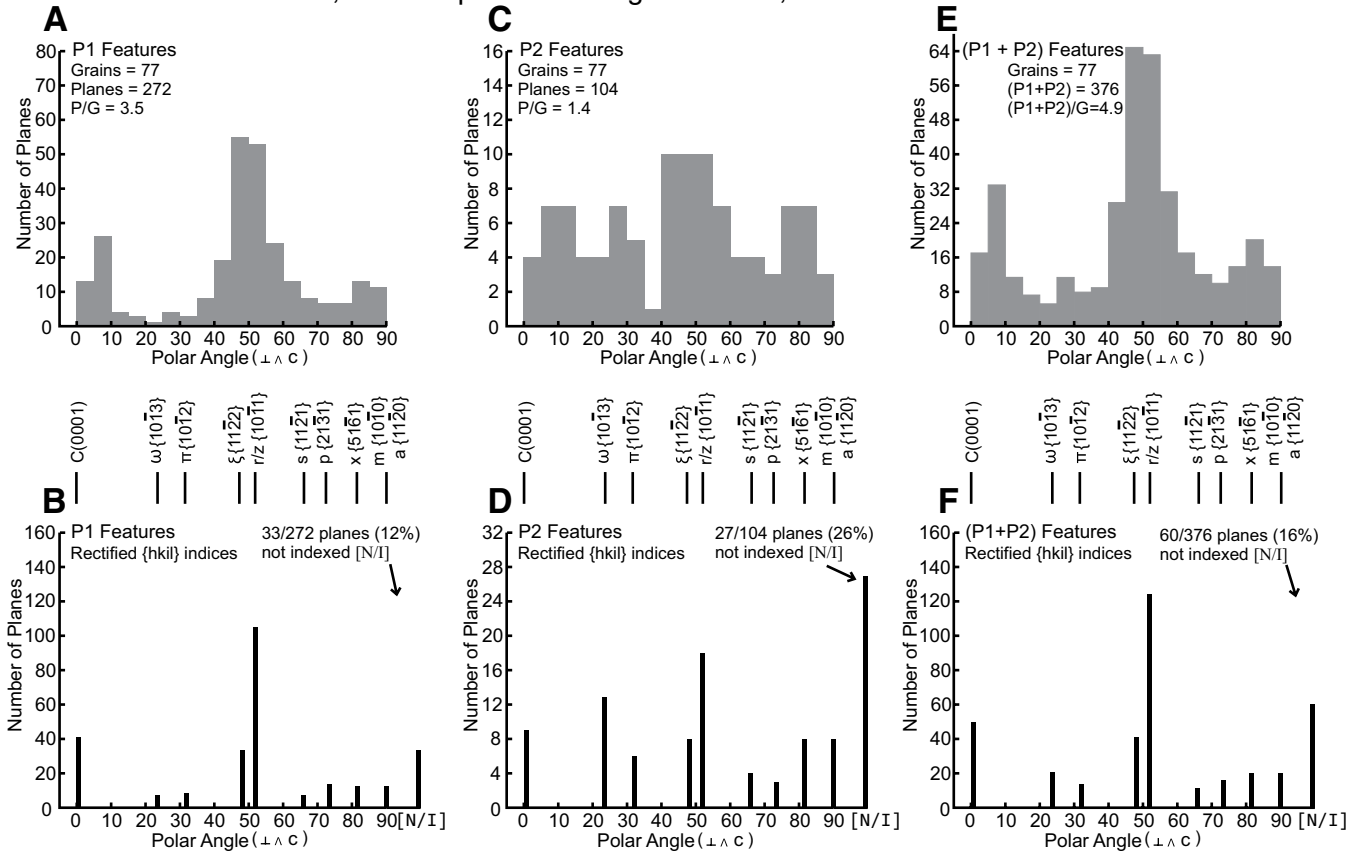


**Figure 16.** Graphs of orientations of planar microstructures in shocked individual quartz grains separated from the microbreccia unit filling the Decorah structure (Sample W-54250; depth interval 80.8–82.3 m.). Histogram plots show frequencies of different angles between quartz *c*-axis and pole to plane for P1 features (cleavage, fractures: A, B), P2 features (possible planar deformation features [PDFs] and other features: C, D), and total features (P1 + P2) (E, F), and total features (P1 + P2) (E, F). Two types of histograms are shown: (1) unmodified frequency data for polar angles (A, C, E), and (2) “rectified” or “spike” plots (B, D, F) derived from a *c*-axis-vertical orientation and allowing identification of {hkil} Miller index values for specific planes (for details, see Grieve et al., 1996; Ferrière et al., 2009). Note, in both types of plots, the strong concentrations of planes corresponding to specific orientations, e.g., (0001) (0°), {10 $\bar{1}$ 3} (23°), {11 $\bar{2}$ 2} (48°), and {10 $\bar{1}$ 1} (52°). Such concentrations are typical and diagnostic for shock-produced deformation features in quartz grains from established impact structures.

tion is a small number of ambiguities in assigning exact {hkil} values to certain closely spaced PM sets, because the accuracy of individual orientation measurements is generally not better than  $\pm 5^\circ$  (e.g., Grieve et al., 1996; Ferrière et al., 2009). In both Decorah samples, a significant number of grains (e.g., ~10% in sample W-52450), which displayed planes at polar angles of 45–55°, produced different but equally good {hkil} matches with the template, regardless of whether these planes were arbitrarily assigned to the forms  $\xi\{11\bar{2}2\}$  (48°) or to  $r/z\{10\bar{1}1\}$  (52°). A smaller number of similar ambiguities were noted with other forms. Choices between these possibilities were made arbitrarily, usually by choosing alternate possibilities in alternate grains. However, the number of grains at issue is relatively small (only a few grains in each measurement group), and regard-

less of how such assignments are made, the different choices produce only small changes in the percentages of the particular planes involved. The overall appearance of the orientation pattern does not change significantly, and the major shock-produced characteristics are preserved.

**Rarity of “Feather Features” at Decorah**

The P2 features at Decorah differ from those at the similar Rock Elm, Wisconsin impact structure (French et al., 2004). At Rock Elm, the features designated as P2 are generally small, healed, quasi-planar fractures, many of which are connected at one end to larger P1 features to form common and distinctive feather features, which are believed to form at relatively low shock pressures (~7–10 GPa) (French et al., 2004; Poelchau and Kenkmann, 2011). At Decorah, most P2 features appear to be genu-

ine PDFs (Fig. 13), which indicate higher shock pressures (>10 GPa; Stöfler and Langenhorst, 1994), while feather features were very rarely observed (e.g., Fig. 14). The difference in apparent shock levels in samples from the two localities could be explained in at least three ways: (1) the difference is a random artifact of the small number of Decorah samples examined; (2) the Rock Elm samples were collected from in-place bedrock located below the final crater floor, where relatively lower shock pressures would be expected (Dence, 1968; Robertson, 1975; Robertson and Grieve, 1977); and (3) the Decorah samples consist of rock fragments and individual quartz grains collected from a probable unit of crater-fill breccia composed of material derived from various locations above the original crater floor. Some of the Decorah material was probably exposed to higher pressures



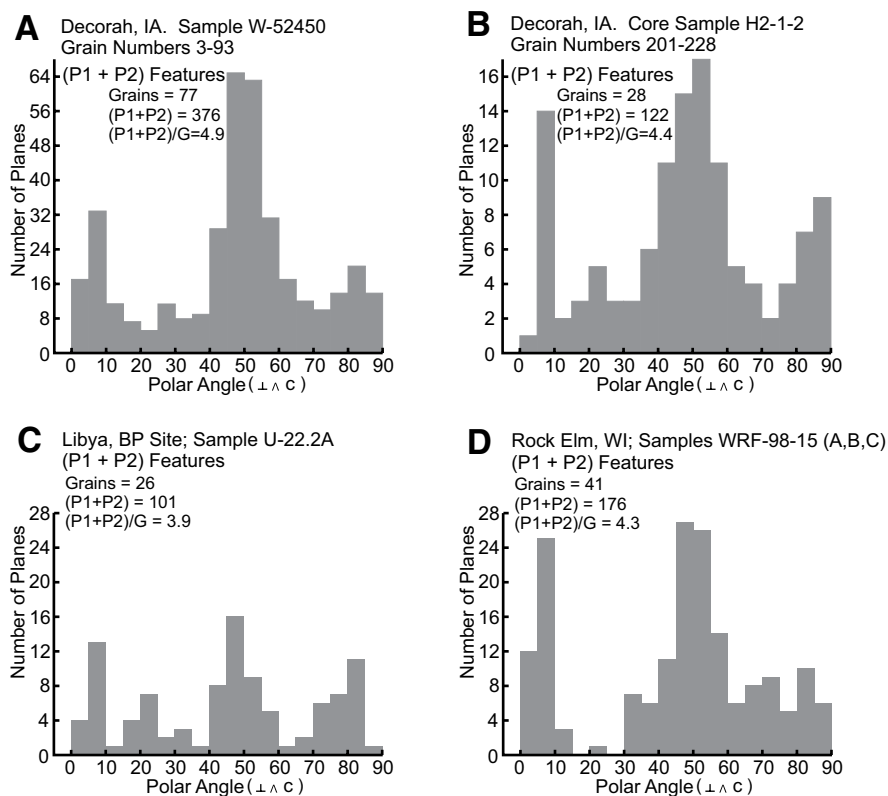


**Figure 17. Graphs of orientations of planar microstructures (P1 + P2 features) in samples from the Decorah structure, Iowa (W-52450 [Fig. 17A] and H2-1-2 [Fig. 17B]) compared with similar plots for quartz grains in samples from established impact structures, the BP site (Libya) (Fig. 17C) (French et al., 1974, Figure 4, plot 1) and Rock Elm, Wisconsin (Fig. 17D) (French and Cordua, 1999, Fig. 3; French et al., 2004, Fig. 4A). (The BP and Rock Elm plots differ slightly from the original publications because they have been constructed by replotting the original data onto the same templates as the Decorah plots.) All plots show the same development of high concentrations of planes corresponding to specific orientations, e.g., {0001} (0°), {10 $\bar{1}$ 3} (23°), {11 $\bar{2}$ 2} (48°), and {10 $\bar{1}$ 1} (52°), which are typical and diagnostic for shock-produced deformation features in quartz grains from established impact structures.**

closer to the impact point, producing numerous grains with definite PDFs and relatively fewer grains with feather features.

### Geological Structure and Comparisons to Other Impact Structures

#### Apparent Absence of a Central Uplift

Our preliminary interpretation of the Decorah structure (Figs. 3 and 18) exhibits several features characteristic of small, deeply eroded meteorite impact structures (e.g., French et al., 2004; French and Koeberl, 2010; Kenkmann et al., 2013, 2014, 2017): a generally circular outline, a shallow-basin shape, and a local sequence of anomalous sediments and/or breccias that truncate and replace the original regional stratigraphy. The presence of diagnostic shock-produced PFs and PDFs in quartz grains from the crater-

fill breccia establishes a strong and convincing similarity between the Decorah structure and numerous other structures generally regarded as the products of meteorite impact events.

However, critical geological information about the structure remains poorly known. Surface exposures are rare and limited to slightly deformed rim rocks and to the uppermost part of the post-impact crater-fill sediments (Winneshiak Shale). Several drill holes provide cuttings samples of the subsurface units (Figs. 3 and 18), but only one basin-centric hole (53572) apparently penetrates the complete thickness of crater breccia and enters the bedrock beneath (Figs. 3, 4, and 18). The two drill holes (52450 and H2) that provided the critical samples for the discovery and analysis of shock-metamorphic features in quartz both bottom in the breccia layer and provide no information about the

crater floor or the sedimentary bedrock units below it. The subsurface character of the Decorah structure is therefore uncertain, and no ground-based geophysical surveys, including gravity and seismic methods, have yet been done. The airborne gravity gradient data (Kass, et al., 2013a, 2013b) clearly demarcate an area of low density consistent with the center of the impact structure, and further modeling with this data set may clarify the depth and three-dimensional configuration of the structure.

Our preliminary interpretation of the Decorah structure (Figs. 3 and 18) shows some significant differences from impact structures of comparable size formed in similar sedimentary targets. The presently preserved Decorah structure apparently lacks a preserved circular, uplifted rim, a condition that may reflect deep erosion of the original structure before deposition of the overlying post-crater sediments. A more striking anomaly is the apparent absence of any structural uplift of the subcrater rocks (Wonewoc, Eau Claire, and Mt. Simon formations) in the center of the structure. This tentative interpretation is based only on the evaluation of cuttings from the single well-hole (53572) that apparently penetrated the crater-fill units and entered into the underlying sedimentary rocks, which appear to be located at approximately the same level as the equivalent units outside the structure (Fig. 3).

The apparent absence of any central uplift in the Decorah structure is surprising. Such uplifts have long been regarded as an integral part of the formation of large (diameter  $>2$  km) impact craters (Dence, 1965; Grieve et al., 1977; Melosh, 1989, Ch. 8), and central uplifts have been identified in nearly all known impact craters in this size range (Grieve and Pilkington, 1996; Kenkmann et al., 2013, 2017), although a few exceptions may exist (Lindström et al., 2005; King et al., 2006; Darlington et al., 2016).

Current cratering models (e.g., Grieve, 1991; Grieve and Pesonen, 1992; Grieve and Pilkington, 1996; Melosh and Ivanov, 1999; Kenkmann et al., 2014) suggest that an impact structure of this size (initial diameter  $\sim 6$  km) in sedimentary rocks would normally develop as a *complex structure*, consisting of a central uplift of underlying target rocks surrounded by an annular depression (commonly filled with impact breccias and overlying sediments), and an outer rim. In such a complex structure, the maximum stratigraphic uplift of subcrater rocks in the central uplift is  $\sim 0.1D$ , where  $D$  is the final crater diameter. This model implies that a central uplift with a maximum stratigraphic uplift of  $\sim 600$  m should have been produced when the Decorah structure formed, but the current limited stratigraphic and drill-core information

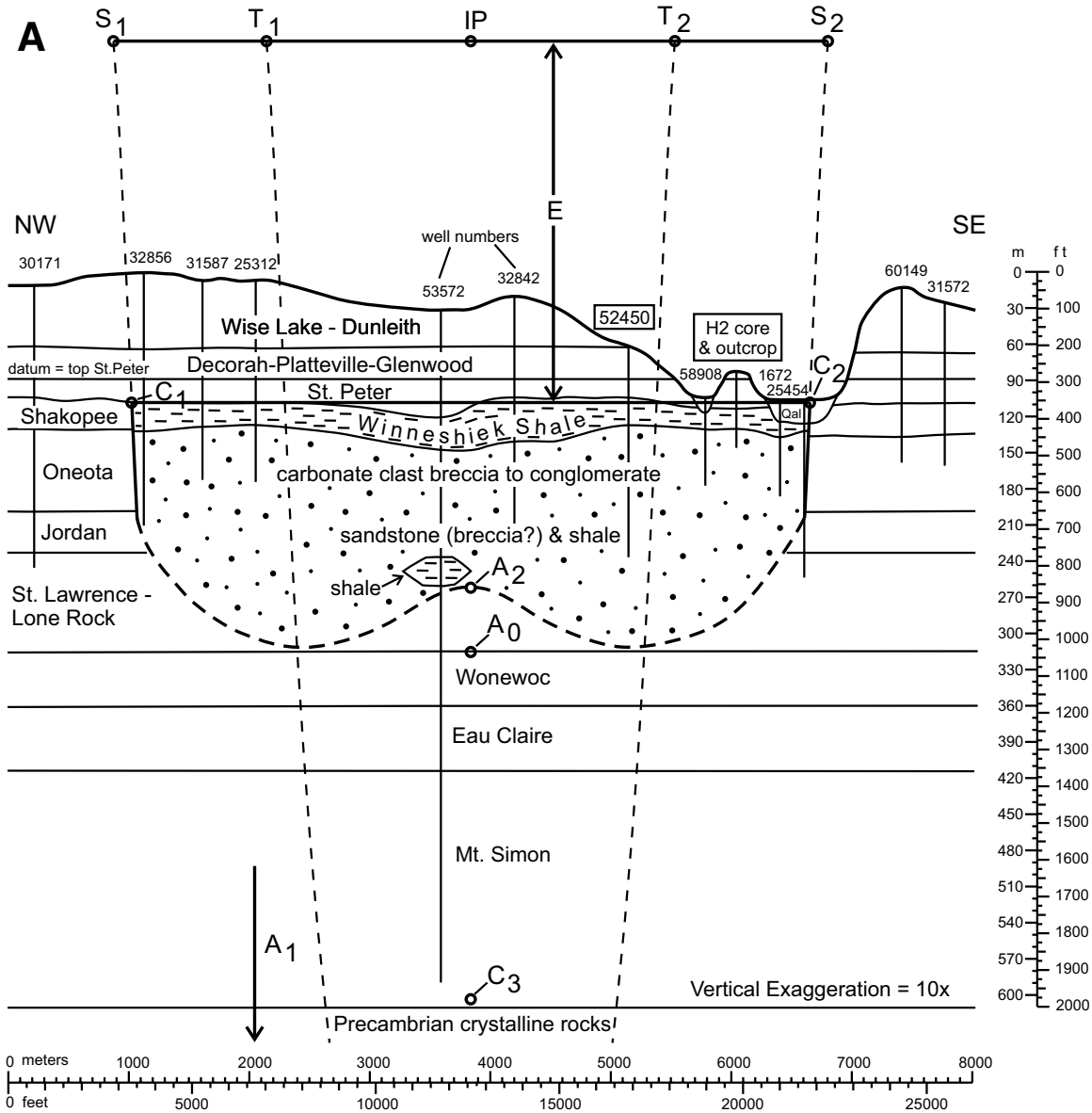
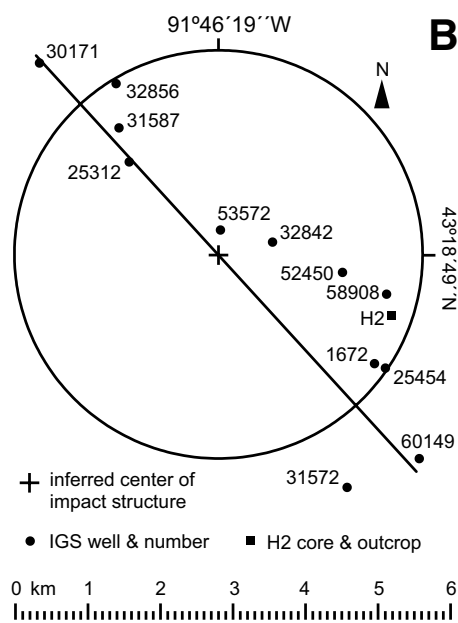


Figure 18. (A) Schematic geological cross section of the Decorah impact structure and pre-impact target stratigraphy, based on drilling results and limited surface exposures (modified from McKay et al., 2011). Vertical exaggeration 10x; datum level set at top of the post-impact St. Peter Sandstone. The section trends parallel to regional strike and has been constructed by projecting stratigraphy determined from multiple wells onto a vertical plane passing in a NW-SE direction through the inferred center of the structure (see Fig. 18B). For simplicity, this reconstruction arbitrarily assumes that the Decorah structure has the general shape of a normal complex crater containing a central uplift of the original crater floor (see Kenkmann et al., 2013, and references therein), although the nature of the subcrater floor and presence of such a central uplift have not been established (see discussion in text: “Apparent Absence of a Central Uplift”). In this cross-section, the Decorah structure is expressed by the presence of an anomalous series of complex and poorly characterized crater-fill units (possible breccias, sandstones, and other sediments, including the uppermost Winneshiek Shale) that fill the preserved lower part of the original crater basin (area within the closed line C<sub>1</sub>-A<sub>2</sub>-C<sub>2</sub>-C<sub>1</sub>) (dark solid line and long dashes) and which interrupt and crosscut the earlier stratigraphic units (St. Lawrence-Lone Rock through Shakopee formations). For comparisons between the original and final impact structures, this figure also includes graphical elements of the impact and the resulting crater, assuming that the structure formed as a typical *complex crater* after the vertical impact of a projectile ~300–400 m in diameter at a velocity of ~15–20 km/sec. At the time of the impact, the original surface (line S<sub>1</sub>-T<sub>1</sub>-IP-T<sub>2</sub>-S<sub>2</sub>) and the *impact point* (IP) were located ~300 m above the present surface. (The intervening sediments were eroded after the impact and before deposition of the St. Peter Sandstone.) Excavation and downward displacement of the target rocks by the initial impact formed a deep, paraboloidal *transient crater* (Dence, 1968; Grieve et al., 1977; Melosh, 1989, Ch. 6) ~4 km in surface diameter and 1.3 km deep, bounded by the line T<sub>1</sub>-A<sub>1</sub>-T<sub>2</sub> (short dashes). The upper part of the transient crater was excavated to a depth of ~600 m from the original surface, and an underlying *displaced zone* extended to a total depth of ~1.3 km from the surface, or deep into the crystalline basement. The point A<sub>0</sub>, originally near the bottom of the upper excavated zone, was driven downward to point A<sub>1</sub>. (Continued on following page.)



**Figure 18 (continued).** In the immediately subsequent *modification stage* of crater formation, the lower part of the transient cavity rebounded upwards, carrying point A<sub>1</sub> up to A<sub>2</sub> and forming a typical central uplift (Kenkmann et al., 2013), while the peripheral parts of the transient crater collapsed inward, enlarging the crater diameter from ~4 km to ~6 km. Deposition of the crater-fill sediments into the resulting basin began at this time and continued for a long period after structural movements of the crater itself had ceased. Line C<sub>1</sub>-C<sub>2</sub> marks the upper boundary of the crater-fill sediments below the St. Peter Sandstone. (B) Plan-view map showing ground locations of wells whose stratigraphic results have been projected onto a NW-SE-trending vertical plane to produce the cross section shown in Figure 18A. Circle approximates the present preserved exposure of the crater-filling Winneshiek Shale and provides an estimate for the current diameter of the present preserved structure, ~5.6 km. Cross indicates the inferred center of the structure.

(Figs. 3 and 18) does not indicate the presence of even a small central uplift, let alone one of this magnitude.

It is unlikely that the absence of a central uplift at Decorah can be explained by post-impact erosion. The central uplifts of more deeply eroded impact structures are generally less prominent and display less stratigraphic uplift than their original maximum, but many complex structures similar to Decorah in size (diameters of 5–7 km) and erosional history preserve stratigraphic uplifts of at least 200–

300 m (e.g., Grieve and Pilkington, 1996; Kenkmann et al., 2014, 2017). The nearby Rock Elm structure, for example, is similar to Decorah in diameter, target rocks, age, and deep erosional level, and still preserves a visible central stratigraphic uplift of at least 200–300 m (French et al., 2004, p. 204).

Current studies of cratering mechanics suggest several possibilities, involving the nature of the impact event or the properties of the target, that might explain the absence of a central uplift at Decorah: (a) an unusually low impact angle (<15° from the horizontal; see Pierazzo and Melosh, 2000; Stickle and Schultz, 2012); (b) a marine impact, involving a target of soft, possibly water-filled, sediments covered by a significant thickness of water (see Ormö and Lindström, 2000; Dypvik and Jansa, 2003; Davison and Collins, 2007; Darlington et al., 2016); and/or (c) immediate major erosion of the newly formed crater (and any original central uplift) by intense post-impact surge currents (see von Dalwigk and Ormö, 2001; Glimsdal et al., 2007).

The existence (or absence) of a central uplift at Decorah is a major issue, not only for the future study of Decorah itself, but for our current understanding of the exact process by which a large number of similar structures have formed. Resolving this problem will probably require extensive local geophysical investigations involving gravity, magnetics, and active seismic methods, ideally supplemented by core drilling through the entire section of crater fill and into the disturbed subcrater rocks.

#### Post-Impact Erosion of the Decorah Structure

The currently preserved Decorah structure (see Figs. 3 and 18) shows virtually no relief under its cover of discomformable St. Peter Sandstone. In particular, there is no indication of a preserved uplifted crater rim or of a thick layer of ejecta surrounding the original crater (Melosh, 1989, Ch. 8; Kenkmann et al., 2013). As a result, neither the thickness of post-Shakopee, pre-impact sediments, nor the vertical height of the impact point above the present surface (which are approximately the same) can be closely estimated, but the information about the present state of the structure can be used to make estimates about the amount of post-impact erosion of the crater and its surroundings.

Current cratering models (Melosh, 1989, Ch. 8; Kenkmann et al., 2013) suggest that removal of the original crater rim and ejecta layer required the erosion of a layer ~300–500 m thick before the eroded structure was covered by the St. Peter Sandstone. By comparison, at the nearby Rock Elm structure there are indications that >300 m of now-eroded sediments younger

than the Prairie du Chien group were present at the time of impact and were subsequently eroded (French et al., 2004, p. 214, and references therein). However, in the Decorah area, such younger pre-impact sediments must have been <300 m thick, or the remaining part of the present bowl-shaped impact structure would not have been preserved. This deep post-impact erosion of the Decorah structure, which represents a hiatus of perhaps 15–20 m.y. (Bunker et al., 1988), developed the major unconformity that now separates the youngest preserved pre-impact rocks (Shakopee Formation) from the oldest post-impact rocks (St. Peter Sandstone).

#### CONCLUSIONS

1. A circular, largely subsurface, basin-shaped feature ~5.6 km in diameter, which displays anomalous geology, has been identified near Decorah, in northeastern Iowa. The surrounding regional geology consists of a uniform section, several hundred m thick, of virtually undeformed cratonic sediments (chiefly sandstones and carbonates) ranging in age from Upper Cambrian to Upper Ordovician and overlying a basement of Mesoproterozoic crystalline rocks.

2. This circular feature (designated here the “Decorah impact structure”) is expressed at the surface by the presence of an unusual shale unit (the Winneshiek Shale) that is restricted to the circular area and has not been found elsewhere in the region. This unit contains a striking Lagerstätte with a variety of well-preserved fossils (Liu et al., 2006, 2017).

3. Surface exposures of the Decorah structure are few, and its subsurface structure is inadequately defined, chiefly from examination of water-well drill-hole cuttings, two short cores, and two small surface exposures. The data available outline an apparently basin-shaped feature that extends from the surface to depths of ~200–300 m, truncating units from the Lower Ordovician Shakopee Formation to the Upper Cambrian St. Lawrence–Lone Rock–Wonewoc formations. The basin and its sedimentary fill are overlain disconformably by the Middle Ordovician St. Peter Sandstone. The structure apparently does not penetrate the underlying Mesoproterozoic crystalline basement rocks.

4. The Decorah structure shows several characteristics that are consistent with formation by meteorite impact: a generally circular outline, a shallow-basin shape, anomalous cross-cutting relations to geological units outside the structure, and a filling of anomalous sediments not present in the regional stratigraphy. However, it lacks evidence for such typical impact features as an uplifted crater rim and a layer of ejecta surrounding the structure.

5. Studies of available drill cuttings and drill core samples indicate that the basin of the Decorah structure is completely filled by a series of sediments, established breccias, and inferred breccias ~200 m thick that are not observed in the sedimentary sequence outside the structure. Several stratigraphically distinct units can be distinguished on the basis of geophysical studies and drill hole cuttings. One upper unit (thickness ~100 m?) is an unusual, poorly sorted, possibly sedimentary, polymict crater-fill breccia composed of fragments of target rock lithologies penetrated by the structure. This unit is overlain by the thinner ( $\leq 27$  m), fine-grained, and finely laminated Winneshiek Shale. Available data suggest that additional lithologies, and a more complex stratigraphy, may also be present in these basin-fill materials.

6. Two samples of the unusual crater-fill breccia, examined by petrographic and petrofabric (Universal Stage) methods, contain significant amounts of single rounded quartz grains, almost certainly derived from underlying Cambrian quartz arenites. A small percentage of these grains ( $\leq 1\%$ ) display multiple sets of parallel planar microstructures of identical appearance and crystallographic orientation (relative to the quartz *c*-axis) to shock-produced features observed in rocks from established meteorite impact structures: planar fractures (cleavage) (“P1 features”) and planar deformation features (PDFs) (“P2 features”). Individual grains typically display as many as 1–5 sets of PFs and 2–4 sets of PDFs, both of which are oriented parallel to specific crystallographic planes in the host quartz, most commonly  $\{0001\}$ ,  $\{11\bar{2}2\}$ , and  $\{10\bar{1}1\}$  (for PFs) and  $\{10\bar{1}1\}$ ,  $\{10\bar{1}3\}$ , and  $\{0001\}$  (for PDFs).

7. Numerous studies by other workers have shown that these planar microstructures are unique and diagnostic shock-metamorphic features, produced by impact-generated shock waves with pressures in the range  $\geq 5$ –10 GPa (for PFs) and 10–20 GPa (for PDFs). They provide convincing evidence that the Decorah structure is a meteorite impact structure. No impact-related products of higher-pressure shock waves (e.g., shock-produced glasses, impact melts) have yet been identified. The identification of the Decorah structure as a meteorite impact feature demonstrates again the potential of petrographic and petrofabric studies, even on small or geologically limited samples, to establish the impact origin of structures that are deeply eroded or largely inaccessible.

8. On the basis of its current diameter, we suggest that the original Decorah structure was a *complex impact crater* with an original diameter of ~6 km. However, unlike virtually all impact structures of comparable size, the Decorah

structure currently shows no evidence for the presence of a structural *central uplift*, an anomaly which probably cannot be resolved without more geological and geophysical studies.

9. Based on impact cratering models, we estimate that the original impact point was located in younger, now-eroded sediments ~300–500 m above the present surface. A similar amount of erosion has therefore occurred post-impact, removing any original upraised crater rim or any ejecta layer that surrounded the original structure. This period of deep erosion, which may have lasted as long as 10–20 m.y., ended with the disconformable deposition of the St. Peter Sandstone over the structure and the surrounding region.

10. The age of the Decorah structure has been estimated from a combination of biostratigraphic and radiometric ages as 460–480 Ma, and a recent chemostratigraphic study of  $\delta^{13}\text{C}_{\text{org}}$  (Bergström et al., 2018) provided a narrower estimate of 464–467 Ma. We therefore suggest, with Bergström et al. (2018), that the Decorah structure may be another member of a growing group of impact structures that apparently represent a “spike” of increased delivery of large and small extraterrestrial bodies to earth during the Middle Ordovician (Schmitz et al., 2001, 2008; Alwmark et al., 2012) following the breakup of the L-chondrite meteorite parent body in the Asteroid Belt at 470 Ma (Korochantseva et al., 2007). We suggest that this hypothesis may be tested by obtaining more precise age dates for the Decorah structure (e.g., by the recovery and analysis of shocked zircons [Cavosie et al., 2010]) or by the recovery of diagnostic extraterrestrial chromite grains from the basin-filling units (Alwmark and Schmitz, 2007; Alwmark et al., 2012).

11. Despite the confident establishment of the origin of the Decorah impact structure, major questions about its characteristics, formation, and history remain. These include: the nature of the subsurface stratigraphy and structure; the presence or absence of an expected central uplift; the precise age of the impact event; the post-impact environment in which the crater-fill breccia and Winneshiek Shale were deposited; the elapsed time (if any) between the end of deposition of the crater-fill breccia and the start of deposition of the Winneshiek Shale; the relative roles of impact processes and post-impact preservation in creating the large and unusual Winneshiek Lagerstätte now preserved within the structure; possible connections between the Decorah event and other mid-Ordovician impact events, and the subsequent geological and biological history of the structure and its surroundings.

12. The information now available about the Decorah structure provides a solid base from

which to plan and execute more sophisticated investigations. The highest priorities for further studies involve the detailed exploration of the structure, its deformed rocks, and its crater-filling units to determine precisely: the present limits of the structure (e.g., diameter, depth, nature of the crater floor); the structural deformation of the deformed target rocks in and around the crater; the lithologies and stratigraphy of the crater-fill materials; and the recognition of other impact-produced lithologies possibly preserved in the structure. Special attention should be given to the Winneshiek Shale: its stratigraphy, its depositional environment, its relations to other impact-produced lithologies in the structure, and the timing of its deposition relative to formation of the structure. These explorations will require cooperative multidisciplinary investigations involving the detailed examination of available cuttings and core samples, further core drilling through the crater fill and into the subcrater rocks, and a range of geophysical studies, especially using gravity, magnetic, and active seismic methods.

13. Further studies of the Decorah structure have the potential to provide specific information on major questions of meteorite impact mechanics, impact crater formation, the effects of impact on the geological environment, and the geological history of the surrounding region. Although many impact structures of comparable size have already been identified, the Decorah structure is particularly important as an unusual example of a possible complex impact structure apparently formed and enclosed entirely in layered sedimentary target rocks, and further studies of Decorah will help illuminate the specific details of such structures and of how they form. In addition, the presence of a striking fossil Lagerstätte within the crater provides an opportunity to study, on a small scale and over a local region, the possible relations between a meteorite impact event and the preservation of local fauna. Finally, further study of the Decorah structure will contribute to understanding its possible relationship to the proposed “spike” of meteorite impact events in the Middle Ordovician and will help illuminate the more general connections between the process of meteorite impact and the geological and biological history of the Earth.

#### ACKNOWLEDGEMENTS

BMF thanks the Department of Paleobiology, Smithsonian Institution, for support as a Research Associate during this study. We thank Sarah Penniston-Dorland (Department of Geology, University of Maryland), Tim Gooding (Department of Mineral Sciences, Smithsonian Institution), and Finnegan Marsh (Department of Paleobiology, Smithsonian Institution) for assistance in producing the photo-

micrographs. RMM and HPL thank Steve and Jane Hildebrand, landowners, for access to outcrop and drill site. Permissions were also provided by the Oneota Country Club, the City of Decorah, Winneshiek County, and Bruening Rock Products. Jean Young (deceased, 2007), friend, Decorah area resident and geologist, was first to recognize unusual strata beneath the St. Peter Formation near Decorah. Phil Kerr (Iowa Geological Survey) provided graphics assistance, Matt Wortel (Department of Earth and Environmental Science, University of Iowa) prepared thin sections, Tony Runkel (Minnesota Geological Survey) provided Minnesota well records, and Ray Anderson discussed impacts. The U.S. Geological Survey StateMap Program supported geologic mapping in Winneshiek County. We also thank David King and Jeffrey Plescia for careful and detailed reviews which significantly improved the manuscript, and Christian Koeberl for editorial handling. Funding for this research was provided by the Iowa Department of Natural Resources and by National Science Foundation grants EAR 0921245 (to HPL, RMM and BJW) and EAR 0922054 (to DEGB).

#### REFERENCES CITED

- Alexopoulos, J.S., Grieve, R.A.F., and Robertson, P.B., 1988, Microscopic lamellar features in quartz: Discriminative characteristics of shock-generated varieties: *Geology*, v. 16, p. 796–799, [https://doi.org/10.1130/0091-7613\(1988\)016<0796:MLDFIQ>2.3.CO;2](https://doi.org/10.1130/0091-7613(1988)016<0796:MLDFIQ>2.3.CO;2).
- Alwmark, C., and Schmitz, B., 2007, Extraterrestrial chromite in the resurge deposits of the early Late Ordovician Lockne crater, central Sweden: *Earth and Planetary Science Letters*, v. 253, p. 291–303, <https://doi.org/10.1016/j.epsl.2006.10.034>.
- Alwmark, C., Schmitz, B., Meier, M.M.M., Baur, H., and Wieler, R., 2012, A global rain of micrometeorites following breakup of the L-chondrite parent body—Evidence from solar wind-implanted Ne in fossil extraterrestrial chromite grains from China: *Meteoritics & Planetary Science*, v. 47, p. 1297–1304, <https://doi.org/10.1111/j.1945-5100.2012.01394.x>.
- Bergström, S.M., Schmitz, B., Liu, H.P., Terfelt, F., and McKay, R.M., 2018, High-resolution  $\delta^{13}\text{C}_{\text{org}}$  chemostratigraphy links the Decorah impact structure and the Winneshiek Konservat-Lagerstätte to the Darriwilian global peak influx of meteorites: *Lethaia*, v. 51, <https://doi.org/10.1111/let.12269>.
- Briggs, D.E.G., Liu, H., McKay, R.M., and Witzke, B.J., 2016, Bivalved arthropods from the Middle Ordovician Winneshiek Lagerstätte, Iowa, USA: *Journal of Paleontology*, v. 89 (for 2015), p. 991–1006, <https://doi.org/10.1017/jpa.2015.76>.
- Bunker, B.J., Witzke, B.J., Watney, W.L., and Ludvigson, G.A., 1988, Phanerozoic history of the central midcontinent, United States, in Sloss, L.L., ed., *Sedimentary Cover—North American Craton, U.S.: Boulder, Colorado, Geological Society of America, The Geology of North America*, v. D-2, p. 243–260, <https://doi.org/10.1130/DNAG-GNA-D2.243>.
- Cavosie, A.J., Quintero, R.R., Radovan, H.A., and Moser, D.E., 2010, A record of ancient cataclysm in modern sand: Shock microstructures in detrital minerals from the Vaal River, Vredefort Dome, South Africa: *Geological Society of America Bulletin*, v. 122, p. 1968–1980, <https://doi.org/10.1130/B30187.1>.
- Chetel, L.M., Singer, B.S., and Simo, T., 2004,  $^{40}\text{Ar}/^{39}\text{Ar}$  geochronology of the Upper Mississippi Valley, Middle and Upper Ordovician Galena Group; sediment accumulation rates and biostratigraphic implications for the history of an epeiric sea: *Geological Society of America Abstracts with Programs*, v. 36, no. 5, p. 75.
- Chetel, L.M., Singer, B.S., and Simo, T., 2005,  $^{40}\text{Ar}/^{39}\text{Ar}$  geochronology of the Upper Mississippi Valley, Middle and Upper Ordovician Galena Group; sediment accumulation rates and biostratigraphic implications for the history of an epeiric sea, in Ludvigson, G.A., and Bunker, B.J., eds., *Facets of the Ordovician Geology of the Upper Mississippi Valley Region: Iowa Geological Survey, Guidebook Series*, no. 24, p. 55–57.
- Cohen, K.M., Finney, S.C., Gibbard, P.L., and Fan, J.X., 2013, The International Commission on Stratigraphy International Chronostratigraphic Chart: Episodes, v. 36, p. 199–204 <http://www.stratigraphy.org/IC-Schart/ChronostratChart2017-02.pdf> (updated version; accessed March 2018).
- Darlington, V., Blenkinsop, T., Dirks, P., Salisbury, J., and Tomkins, A., 2016, The Lawn Hill annulus: An Ordovician meteorite impact into water-saturated dolomite: *Meteoritics & Planetary Science*, v. 51, p. 2416–2440, <https://doi.org/10.1111/maps.12734>.
- Davison, T., and Collins, G.S., 2007, The effect of the oceans on terrestrial crater size-frequency distribution: Insight from numerical modeling: *Meteoritics & Planetary Science*, v. 42, p. 1915–1927, <https://doi.org/10.1111/j.1945-5100.2007.tb00550.x>.
- Dence, M.R., 1965, The extraterrestrial origin of Canadian craters: *Annals of the New York Academy of Sciences*, v. 123, p. 941–969, <https://doi.org/10.1111/j.1749-6632.1965.tb20411.x>.
- Dence, M.R., 1968, Shock zoning at Canadian craters: Petrography and structural implications: in French, B.M., and Short, N.M. eds., *Shock metamorphism of natural materials*: Baltimore, Maryland, Mono Book Corporation, p. 169–184.
- Dence, M.R., Innes, M.J.S., and Robertson, P.B., 1968, Recent geological and geophysical studies of Canadian craters, in French, B.M., and Short, N.M., eds., *Shock metamorphism of natural materials*: Baltimore, Maryland, Mono Book Corporation, p. 339–362.
- Drenth, B.J., Anderson, R.R., Schulz, K.J., Feinberg, J.M., Chandler, V.W., and Cannon, W.F., 2015, What lies beneath; geophysical mapping of a concealed Precambrian intrusive complex along the Iowa-Minnesota border: *Canadian Journal of Earth Sciences*, v. 52, no. 5, p. 279–293.
- Dypvik, H., and Jansa, L.F., 2003, Sedimentary signatures and processes during marine bolide impacts: a review: *Sedimentary Geology*, v. 161, p. 309–337, [https://doi.org/10.1016/S0037-0738\(03\)00135-0](https://doi.org/10.1016/S0037-0738(03)00135-0).
- Earth Impact Database, 2016, University of New Brunswick, Fredericton, New Brunswick, Canada: <http://www.pasc.net/EarthImpactDatabase/index.html> (accessed December 2016).
- Engelhardt, W.v., and Bertsch, W., 1969, Shock induced planar deformation structures in quartz from the Ries crater, Germany: *Contributions to Mineralogy and Petrology*, v. 20, p. 203–234, <https://doi.org/10.1007/BF00377477>.
- Ferrière, L., Morrow, J.R., Amgaa, T., and Koeberl, C., 2009, Systematic study of universal-stage measurements of planar deformation features in shocked quartz: Implications for statistical significance and representation of results: *Meteoritics & Planetary Science*, v. 44, p. 925–940, <https://doi.org/10.1111/j.1945-5100.2009.tb00778.x>.
- French, B.M., 1998, Traces of catastrophe: a handbook of shock-metamorphic effects in terrestrial meteorite impact craters: Houston, Texas, Lunar and Planetary Institute, Contribution CB-954, 120 p. (<http://www.lpi.usra.edu/publications/books/>).
- French, B.M., 2004, The importance of being cratered: The new role of meteorite impact as a normal geological process: *Meteoritics & Planetary Science*, v. 39, p. 169–197, <https://doi.org/10.1111/j.1945-5100.2004.tb00335.x>.
- French, B.M., and Cordua, W.C., 1999, Intense fracturing of quartz at the Rock Elm, Wisconsin “cryptoexplosion” structure: Evidence for meteorite impact [abs.]: Lunar and Planetary Science Conference, 30th, Houston, Texas, Abstracts, CD-ROM, no. 1123.
- French, B.M., and Koeberl, C., 2010, The convincing identification of meteorite impact structures: What works, what doesn’t, and why: *Earth-Science Reviews*, v. 98, p. 123–170, <https://doi.org/10.1016/j.earscirev.2009.10.009>.
- French, B.M., and Short, N.M., eds., 1968, *Shock metamorphism of natural materials*: Baltimore, Maryland, Mono Book Corp., 644 p.
- French, B.M., Underwood, J.R., Jr., and Fisk, E.P., 1974, Shock-metamorphic features in two meteorite impact structures, southeastern Libya: *Geological Society of America Bulletin*, v. 85, p. 1425–1428, [https://doi.org/10.1130/0016-7606\(1974\)85<1425:SFITMI>2.0.CO;2](https://doi.org/10.1130/0016-7606(1974)85<1425:SFITMI>2.0.CO;2).
- French, B.M., Cordua, W., and Plescia, J.B., 2004, The Rock Elm meteorite impact structure, Wisconsin: Geology and shock-metamorphic effects in quartz: *Geological Society of America Bulletin*, v. 116, p. 200–218, <https://doi.org/10.1130/B25207.1>.
- Glimsdal, S., Pedersen, G.K., Langtangen, H.P., Shuvalov, V., and Dypvik, H., 2007, Tsunami generation and propagation from the Mjølner asteroid impact: *Meteoritics & Planetary Science*, v. 42, p. 1473–1493, <https://doi.org/10.1111/j.1945-5100.2007.tb00586.x>.
- Grieve, R.A.F., 1987, Terrestrial impact structures: Annual Review of Earth and Planetary Sciences, v. 15, p. 245–270, <https://doi.org/10.1146/annurev.ea.15.050187.001333>.
- Grieve, R.A.F., 1991, Terrestrial impact: the record in the rocks: *Meteoritics*, v. 26, p. 175–194, <https://doi.org/10.1111/j.1945-5100.1991.tb01038.x>.
- Grieve, R.A.F., 1997, Extraterrestrial impact events: The record in the rocks and the stratigraphic column: *Palaeogeography, Palaeoclimatology, Palaeoecology*, v. 132, p. 5–23, [https://doi.org/10.1016/S0031-0182\(97\)00058-8](https://doi.org/10.1016/S0031-0182(97)00058-8).
- Grieve, R.A.F., 1998, Extraterrestrial impacts on the earth: the evidence and the consequences, in Grady, M.M., Hutchinson, R., McCall, G.J.H., and Rothery, D., eds., *Meteorites: Flux with time and impact effects*: London, Geological Society Special Publication 140, p. 105–131, <https://doi.org/10.1144/GSL.SP.1998.140.01.10>.
- Grieve, R.A.F., 2001, The terrestrial cratering record, in Peucker-Ehrenbrink, B., and Schmitz, B., eds., *Accretion of extraterrestrial matter throughout Earth’s history*: New York, Kluwer Academic/Plenum Publishers, p. 379–402, [https://doi.org/10.1007/978-1-4419-8694-8\\_19](https://doi.org/10.1007/978-1-4419-8694-8_19).
- Grieve, R.A.F., and Pesonen, L.J., 1992, The terrestrial impact cratering record: Tectonophysics, v. 216, p. 1–30, [https://doi.org/10.1016/0040-1951\(92\)90152-V](https://doi.org/10.1016/0040-1951(92)90152-V).
- Grieve, R.A.F., and Pilkington, M., 1996, The signature of terrestrial impacts: *AGSO Journal of Australian Geology & Geophysics*, v. 16, p. 399–420.
- Grieve, R.A.F., Dence, M.R., and Robertson, P.B., 1977, Cratering process: As interpreted from the occurrence of impact melts, in Roddy, D.J., Pepin, R.O., and Merrill, R.B., eds., *Impact and explosion cratering*: New York, Pergamon Press, p. 791–814.
- Grieve, R.A.F., Langenhorst, F., and Stöffler, D., 1996, Shock metamorphism of quartz in nature and experiment: II. Significance in geosciences: *Meteoritics & Planetary Science*, v. 31, p. 6–35, <https://doi.org/10.1111/j.1945-5100.1996.tb02049.x>.
- Hawkins, A.D., Liu, H.P., Briggs, D.E.G., Muscente, A.D., McKay, R.M., Witzke, B.J., and Xiao, S., 2018, Taphonomy and biological affinity of three-dimensional phosphatized bromalites from the Middle Ordovician Winneshiek Lagerstätte, northeastern Iowa, USA: *Palaio*, v. 33, p. 1–15, <https://doi.org/10.2110/palo.2017.053>.
- Hergarten, S., and Kenkmann, T., 2015, The number of impact craters on Earth: Any room for further discoveries? *Earth and Planetary Science Letters*, v. 425, p. 187–192, <https://doi.org/10.1016/j.epsl.2015.06.009>.
- Huber, M.S., Ferrière, L., Losiak, A., and Koeberl, C., 2011, ANIE: A mathematical algorithm for automated indexing of Planar Deformation Features in shocked quartz: *Meteoritics & Planetary Science*, v. 46, p. 1418–1424, <https://doi.org/10.1111/j.1945-5100.2011.01234.x>.
- Jourdan, F., and Reimold, U.W., eds., 2012, *Impact!: Elements*, Special issue, v. 8, no. 1, 60 p.
- Kass, M.A., Bedrosian, P.A., Drenth, B.J., Bloss, B.R., McKay, R.M., Liu, H., French, B.M., and Witzke, B.J., 2013a, Modeling and inversion results from airborne geophysics over a buried impact structure in Decorah, Iowa, USA: *Geological Society of America Abstracts with Programs*, v. 45, no. 7, p. 485.
- Kass, M.A., Bedrosian, P.A., Drenth, B.J., Bloss, B.R., McKay, R.M., Liu, H., French, B.M., and Witzke, B.J., 2013b, Geophysical signatures and modeling results from a buried impact structure in Decorah, Iowa, USA:



- American Geophysical Union Fall Meeting (December 2013), Abstract P34C-04.
- Kenkmann, T., Collins, G.S., and Wünnemann, K., 2013, The modification stage of crater formation, *in* Osinski, G.R. and Pierazzo, E., eds., *Impact Cratering: Processes and Products*: Chichester, UK, Wiley-Blackwell, p. 60–75.
- Kenkmann, T., Poelchau, M.H., and Wulf, G., 2014, Structural geology of impact craters: *Journal of Structural Geology*, v. 62, p. 156–182, <https://doi.org/10.1016/j.jsg.2014.01.015>.
- Kenkmann, T., Sturm, S., Krüger, T., and Salameh, E., 2017, The structural inventory of a small impact crater: Jebel Waqf as Suwwan, Jordan: *Meteoritics & Planetary Science*, v. 52, p. 1351–1370, <https://doi.org/10.1111/maps.12823>.
- King, D.T., Jr., Ormó, J., Petruny, L.W., and Neathery, T.L., 2006, Role of water in the formation of the Late Cretaceous Wetumpka impact structure, inner Gulf Coastal Plain of Alabama, USA: *Meteoritics & Planetary Science*, v. 41, p. 1625–1631, <https://doi.org/10.1111/j.1945-5100.2006.tb00440.x>.
- Koerberl, C., 2014, The geochemistry and cosmochemistry of impacts, *in* *Treatise on geochemistry*, 2nd ed.: Elsevier, Reference Module in Earth Systems and Environmental Sciences, p. 73–118, <https://doi.org/10.1016/B978-0-08-095975-7.00130-3>.
- Kolata, D.R., Huff, W.D., and Bergström, S.M., 1996, Ordovician K-bentonites of eastern North America: *Geological Society of America Special Paper* 313, 84 p., <https://doi.org/10.1130/SPE313>.
- Korochantseva, E.K., Trieloff, M., Lorenz, C.A., Buykin, A.L., Ivanova, M.A., Schwarz, W.H., Hopp, J., and Jessberger, E., 2007, L-chondrite asteroid breakup tied to Ordovician meteorite shower by multiple isochron <sup>40</sup>Ar-<sup>39</sup>Ar dating: *Meteoritics & Planetary Science*, v. 42, p. 113–130, <https://doi.org/10.1111/j.1945-5100.2007.tb00221.x>.
- Lamsdell, J.C., Briggs, D.E.G., Liu, H.P., Witzke, B.J., and McKay, R.M., 2015a, A new Ordovician arthropod from the Winneshiek Lagerstätte of Iowa (USA) reveals the ground plan of eurypterids and chasmatsipidids: *The Science of Nature*, v. 102, no. 63, p. 1–8.
- Lamsdell, J.C., Briggs, D.E.G., Liu, H.P., Witzke, B.J., and McKay, R.M., 2015b, The oldest described eurypterid: a giant Middle Ordovician (Darrivillan) megalograptid from the Winneshiek Lagerstätte of Iowa: *BMC Evolutionary Biology*, v. 15, no. 169, p. 1–31.
- Lindström, M., Ormó, J., Sturkell, E., and von Dalwigk, I., 2005, The Lockne Crater: Revision and reassessment of structure and impact stratigraphy, *in* Koerberl, C. and Henkel, H. eds., *Impact Tectonics*: New York, Springer Publishers, p. 357–388, [https://doi.org/10.1007/3-540-27548-7\\_14](https://doi.org/10.1007/3-540-27548-7_14).
- Liu, H.P., McKay, R.M., Young, J.N., Witzke, B.J., McVey, K.J., and Liu, X., 2006, A new Lagerstätte from the Middle Ordovician St. Peter Formation in northeast Iowa, USA: *Geology*, v. 34, p. 969–972, <https://doi.org/10.1130/G22911A.1>.
- Liu, H.P., McKay, R.M., Young, J.N., Witzke, B.J., McVey, K.J., and Liu, X., 2007a, The Winneshiek Lagerstätte: *Acta Palaeontologica Sinica*, v. 46, supplement, p. 282–285.
- Liu, H.P., Witzke, B.J., Young, J.N., and McKay, R.M., 2007b, Conodonts from the Winneshiek Lagerstätte, St. Peter Sandstone (Ordovician) of northeast Iowa: *Geological Society of America Abstracts with Programs*, v. 39, no. 9, p. 63.
- Liu, H.P., McKay, R.M., Witzke, B.J., and Briggs, D.E.G., 2009, The Winneshiek Lagerstätte, Iowa, USA and its depositional environments: *Geological Journal of China Universities*, v. 15, p. 285–295 (in Chinese with English summary).
- Liu, H., Briggs, D.E.G., McKay, R.M., and Witzke, B.J., 2013, The Middle Ordovician Winneshiek Lagerstätte—An unusual setting for exceptional preservation: *Geological Society of America Abstracts with Programs*, v. 45, no. 7, p. 454.
- Liu, H.P., Bergström, S.M., Witzke, B.J., Briggs, D.E.G., McKay, R.M., and Ferretti, A., 2017, Exceptionally preserved conodont apparatuses with giant jaw-like elements from the Middle Ordovician Winneshiek Konservat-Lagerstätte, Iowa, USA: *Journal of Paleontology*, v. 91, p. 493–511, <https://doi.org/10.1017/jpa.2016.155>.
- Losiak, A., Golebiowska, I., Ferrière, L., Wojciechowski, J., Huber, M.S., and Koerberl, C., 2016, WIP: A Web-based program for indexing planar features in quartz grains and its usage: *Meteoritics & Planetary Science*, v. 51, p. 647–662, <https://doi.org/10.1111/maps.12614>.
- Lowman, P.D., 2002, *Exploring space, exploring Earth: New understanding of the Earth from space research*: New York, Cambridge University Press, 362 p.
- Ludvigson, G.A., and Bunker, B.J., eds., 2005, *Facets of the Ordovician Geology of the Upper Mississippi Valley Region*: Iowa Geological Survey, Guidebook Series, no. 24, 129 p.
- McKay, R.M., 1988, Stratigraphy and lithofacies of the Dresbachian (Upper Cambrian) Eau Claire Formation in the subsurface of eastern Iowa, *in* Ludvigson, G.A., and Bunker, B.J., eds., *New perspectives on the Paleozoic history of the Upper Mississippi Valley*: Iowa Geological Survey, Guidebook, no. 8, a guidebook for the 18th Annual Field Conference of the Great Lakes Section, Society of Economic Paleontologists and Mineralogists, p. 33–53.
- McKay, R.M., 1993, Selected aspects of Lower Ordovician and Upper Cambrian geology in Allamakee and northern Clayton counties: *Geological Society of Iowa, Guidebook* 57, 61 p.
- McKay, R.M., Liu, H., Witzke, B.J., and French, B.M., 2010, Geological setting of the Winneshiek Lagerstätte—Decorah, Iowa: *Geological Society of America Abstracts with Programs*, v. 42, no. 2, p. 89.
- McKay, R.M., Liu, H., Witzke, B.J., French, B.M., and Briggs, D.E.G., 2011, Preservation of the Middle Ordovician Winneshiek Shale in a probable impact crater: *Geological Society of America Abstracts with Programs*, v. 43, no. 5, p. 189.
- Melosh, H.J., 1989, *Impact cratering: A geological process*: Oxford, U.K., Oxford University Press, 245 p.
- Melosh, H.J., and Ivanov, B.A., 1999, Impact crater collapse: *Annual Review of Earth and Planetary Sciences*, v. 27, p. 385–415, <https://doi.org/10.1146/annurev.earth.27.1.385>.
- Montanari, A., and Koerberl, C., 2000, *Impact stratigraphy: the Italian record*: Notes in Earth Sciences, v. 93, New York, Springer Publishers, 364 p.
- Nowak, H., Harvey, T.H.P., Liu, H.P., McKay, R.M., Zippi, P.A., Campbell, D.H., and Servais, T., 2017, Filamentous eukaryotic algae with a possible cladophoralean affinity from the Middle Ordovician Winneshiek Lagerstätte in Iowa, USA: *Geobios*, v. 50, p. 303–309, <https://doi.org/10.1016/j.geobios.2017.06.005>.
- Nowak, H., Harvey, T.H.P., Liu, H.P., McKay, R.M., and Servais, T., 2018, Exceptionally preserved arthropodan microfossils from the Middle Ordovician Winneshiek Lagerstätte, Iowa, USA: *Leaitha*, v. 51, p. 267–276, <https://doi.org/10.1111/let.12236>.
- Odom, I.E., 1975, Feldspar-grain size relations in Cambrian arenites, upper Mississippi Valley: *Journal of Sedimentary Petrology*, v. 45, p. 636–650.
- Ormó, J., and Lindström, M., 2000, When a cosmic impact strikes the sea bed: *Geological Magazine*, v. 137, p. 67–80, <https://doi.org/10.1017/S0016756800003538>.
- Osinski, G.R., and Pierazzo, E., eds., 2013, *Impact cratering: Processes and products*: Chichester, UK, Wiley-Blackwell, 316 p.
- Pierazzo, E., and Melosh, H.J., 2000, Understanding oblique impacts from experiments, observations, and modeling: *Annual Review of Earth and Planetary Sciences*, v. 28, p. 141–167, <https://doi.org/10.1146/annurev.earth.28.1.141>.
- Poelchau, M.H., and Kenkmann, T., 2011, Feather-features: A low-shock-pressure indicator in quartz: *Journal of Geophysical Research*, v. 116, B02201, 13 p. <https://doi.org/10.1029/2010JB007803>.
- Prior, J.C., 1991, *Landforms of Iowa*: Iowa City, Iowa, University of Iowa Press, 154 p.
- Robertson, P.B., 1975, Zones of shock metamorphism at the Charlevoix impact structure, Quebec: *Geological Society of America Bulletin*, v. 86, p. 1630–1638, [https://doi.org/10.1130/0016-7606\(1975\)86<1630:ZOSMAT>2.0.CO;2](https://doi.org/10.1130/0016-7606(1975)86<1630:ZOSMAT>2.0.CO;2).
- Robertson, P.B., and Grieve, R.A.F., 1977, Shock attenuation in terrestrial impact structures, *in* Roddy, D.J., Pepin, R.O., and Merrill, R.B., eds., *Impact and explosion cratering: Planetary and terrestrial implications*: New York, Pergamon, p. 687–702.
- Robertson, P.B., Dence, M.F., and Vos, M.A., 1968, Deformation in rock-forming minerals from Canadian craters, *in* French, B.M., and Short, N.M., eds., *Shock metamorphism of natural materials*: Baltimore, Maryland, Mono Book Corporation, p. 433–452.
- Runkel, A.C., 1996, *Bedrock geology of Houston County, Minnesota*: Minnesota Geological Survey Open-File Report 96-4, 3 pls., scale 1:100,000; text, 13 p.
- Runkel, A.C., McKay, R.M., and Palmer, A.R., 1998, Origin of a classic cratonic sheet sandstone; stratigraphy across the Sauk II–Sauk III boundary in the Upper Mississippi Valley: *Geological Society of America Bulletin*, v. 110, p. 188–210, [https://doi.org/10.1130/0016-7606\(1998\)110<0188:OOACCS>2.3.CO;2](https://doi.org/10.1130/0016-7606(1998)110<0188:OOACCS>2.3.CO;2).
- Runkel, A.C., Miller, J.F., McKay, R.M., Palmer, A.R., and Taylor, J.F., 2007, High-resolution sequence stratigraphy of lower Paleozoic sheet sandstones in central North America: The role of special conditions of cratonic interiors in development of stratal architecture: *Geological Society of America Bulletin*, v. 119, p. 860–881, <https://doi.org/10.1130/B26117.1>.
- Runkel, A.C., Miller, J.F., McKay, R.M., Palmer, A.R., and Taylor, J.F., 2008, The record of time in cratonic interior strata: does exceptionally slow subsidence necessarily result in exceptionally poor stratigraphic completeness? *in* Pratt, B.R., and Holmden, C., eds., *Dynamics of Epicratic Seas*: Geological Association of Canada, Special Paper 48, p. 341–362.
- Schmitz, B., Tassanari, M., and Peucker-Ehrenbrink, B., 2001, A rain of ordinary chondrite meteorites in the Early Ordovician: *Earth and Planetary Science Letters*, v. 194, p. 1–15, [https://doi.org/10.1016/S0012-821X\(01\)00559-3](https://doi.org/10.1016/S0012-821X(01)00559-3).
- Schmitz, B.S., Harper, D.A.T., Peucker-Ehrenbrink, B., Stouge, S., Alwmark, C., Cronholm, A., Bergström, S.M., Tassanari, M., and Xiaofeng, W., 2008, Asteroid breakup linked to the Great Ordovician Biodiversification Event: *Nature Geoscience*, v. 1, p. 49–52, <https://doi.org/10.1038/ngeo.2007.37>.
- Schulte, P., et al., 2010, The Chicxulub asteroid impact and mass extinction at the Cretaceous–Paleogene boundary: *Science*, v. 327, p. 1214–1218, <https://doi.org/10.1126/science.1177265>.
- Smith, G.L., and Clark, D.L., 1996, Conodonts of the Lower Ordovician Prairie du Chien Group of Wisconsin and Minnesota: *Micropaleontology*, v. 42, no. 4, p. 363–373, <https://doi.org/10.2307/1485958>.
- Smith, M.E., Singer, B.S., and Simo, T., 2011, Tiered interpolation of radioisotopic and biostratigraphic geochronology resolves the tempo of the Ordovician icehouse to greenhouse transition: *Geological Society of America Abstracts with Programs*, v. 43, no. 5, p. 568.
- Spry, A., 1969, *Metamorphic textures*: New York, Pergamon Press, 350 p.
- Stewart, S.A., 2011, Estimates of yet-to-find impact crater population on Earth: *Journal of the Geological Society*, v. 168, p. 1–14, <https://doi.org/10.1144/0016-76492010-006>.
- Stickle, A., and Schultz, P.H., 2012, Oblique hypervelocity impacts into layered targets: *Journal of Geophysical Research*, v. 117, no. E7, <https://doi.org/10.10292011JE004043>.
- Stöffler, D., and Langenhorst, F., 1994, Shock metamorphism of quartz in nature and experiment: I. Basic observation and theory: *Meteoritics & Planetary Science*, v. 29, p. 155–181, <https://doi.org/10.1111/j.1945-5100.2006.tb00448.x>.
- Tagle, R., and Hecht, L., 2006, Geochemical identification of projectiles in impact rocks: *Meteoritics & Planetary Science*, v. 41, p. 1721–1735, <https://doi.org/10.1111/j.1945-5100.2006.tb00448.x>.
- Trefil, J.S., and Raup, D.M., 1990, Crater taphonomy and bombardment rates in the Phanerozoic: *The Journal of Geology*, v. 98, p. 385–398, <https://doi.org/10.1086/j629411>.

- Vernon, R.H., 2004, A practical guide to rock microstructure: New York, Cambridge University Press, 594 p, <https://doi.org/10.1017/CBO9780511807206>.
- von Dalwigk, L., and Ormö, J., 2001, Formation of resurge gullies at impacts at sea: The Lockne crater, Sweden: *Meteoritics & Planetary Science*, v. 36, p. 359–369, <https://doi.org/10.1111/j.1945-5100.2001.tb01879.x>.
- Whitehead, J., Spray, J.G., and Grieve, R.A.F., 2002, Origin of “toasted” quartz in terrestrial impact structures: *Geology*, v. 30, p. 431–434, [https://doi.org/10.1130/0091-7613\(2002\)030<0431:OOTQIT>2.0.CO;2](https://doi.org/10.1130/0091-7613(2002)030<0431:OOTQIT>2.0.CO;2).
- Witzke, B.J., and Glenister, B.F., 1987, The Ordovician sequence in the Guttenberg area, northeast Iowa, *in* Biggs, D.L., ed., North Central Section of the Geological Society of America: Boulder, Colorado, Geological Society of America, Centennial Field Guide, v. 3, p. 93–96, <https://doi.org/10.1130/0-8137-5403-8.93>.
- Witzke, B.J., and McKay, R.M., 1987, Cambrian and Ordovician stratigraphy in the Lansing area, northeastern Iowa, *in* Biggs, D.L., ed., North Central Section of the Geological Society of America: Boulder, Colorado, Geological Society of America, Centennial Field Guide, v. 3, p. 81–87, <https://doi.org/10.1130/0-8137-5403-8.81>.
- Witzke, B.J., McKay, R.M., Liu, H.P., and Briggs, D.E.G., 2011, The Middle Ordovician Winneshiek Shale of northeast Iowa—Correlation and paleogeographic implications: *Geological Society of America Abstracts with Programs*, v. 43, no. 5, p. 315.
- Wolter, C.F., McKay, R.M., Liu, H., Bounk, M.J., and Libra, R.D., 2011, Geologic Mapping For Water Quality Projects in the Upper Iowa River Watershed: Iowa Geological Survey, Technical Information Series, no. 54, 34 p.

SCIENCE EDITOR: AARON J. CAVOSIE  
ASSOCIATE EDITOR: CHRISTIAN KOEBERL

MANUSCRIPT RECEIVED 7 SEPTEMBER 2017  
REVISED MANUSCRIPT RECEIVED 1 MAY 2018  
MANUSCRIPT ACCEPTED 19 JUNE 2018

Printed in the USA